Spring 2015

Hybrid power system for Micro Air Vehicles

Bakytgul Khaday
Purdue University

Graduate School Form 30
Updated 1/15/2015

PURDUE UNIVERSITY
GRADUATE SCHOOL
Thesis/Dissertation Acceptance

This is to certify that the thesis/dissertation prepared

By Bakytgul Khaday

Entitled

HYBRID POWER SYSTEM FOR MICRO AIR VEHICLES

For the degree of Master of Science

Is approved by the final examining committee:

Eric T. Matson
Chair

J. Eric Dietz
Co-chair

J Michael Jacob
Co-chair

To the best of my knowledge and as understood by the student in the Thesis/Dissertation Agreement, Publication Delay, and Certification Disclaimer (Graduate School Form 32), this thesis/dissertation adheres to the provisions of Purdue University's "Policy of Integrity in Research" and the use of copyright material.

Approved by Major Professor(s): Eric T. Matson

Approved by: Jeffrey L. Whitten 4/8/2015

Head of the Departmental Graduate Program Date

HYBRID POWER SYSTEM FOR MICRO AIR VEHICLES

A Thesis

Submitted to the Faculty

of

Purdue University

by

Bakytgul Khaday

In Partial Fulfillment of the

Requirements for the Degree

of

Master of Science

May 2015

Purdue University

West Lafayette, Indiana

Dedicated to my parents, Khaday Belchirbay and Sharipa Akhmad, my family, my love Bakhtiyar Suleimenov, and my friends.

ACKNOWLEDGMENTS

I wish to gratefully acknowledge my thesis committee, my labmate and friend Yongho Kim, and Professor Athula Kulatunga for their insightful comments and guidance and for their support and encouragement. Special thanks to Dr. Eric Matson for giving me the opportunity to conduct this research.

TABLE OF CONTENTS

Page

LIST OF TABLES

LIST OF FIGURES

Figure Page

SYMBOLS

m	mass (g)
V	voltage (V)
I	current (A)
R	resistance (Ohm)
t	time (sec)
C	capacitance (F)

ABBREVIATIONS

MAV	Micro Air Vehicle
SCAP	Supercapacitor
PCB	Printed Circuit Board

GLOSSARY

DC-to-DC Converter	an electronic circuit which converts one direct-current voltage into another, consisting of an inverter followed by a step-up or step-down transformer and rectifier (thefreedictionary)
Direct Current (DC)	a continuous electric current that flows in one direction only, without substantial variation in magnitude (thefreedictionary)
Hybrid Power System	combine two or more modes of electricity generation, usually using renewable technologies such as solar photovoltaic (PV) and wind turbines. Hybrid systems provide a high level of energy security through the mix of generation methods, and often will incorporate a storage system (battery, fuel cell) or small fossil fueled generator to ensure maximum supply reliability and security (thefreedictionary)
MAV	a micro air vehicle (MAV), or micro aerial vehicle, is a class of unmanned aerial vehicles (UAV) that has a size restriction and may be autonomous. Modern craft can be as small as 15 centimetres (thefreedictionary)

Ragone Chart	the Ragone Chart (also called Ragone plot) is a chart used for performance comparison of various energy storing devices. On such a chart the values of energy density (in Wh/kg) are plotted versus power density (in W/kg). Both axes are logarithmic, which allows comparing performance of very different devices (for example extremely high, and extremely low power) (thefreedictionary)

ABSTRACT

Khaday, Bakytgul M.S., Purdue University, May 2015. Hybrid power system for micro air vehicles. Major Professor: Eric T. Matson.

Today Micro Air Vehicles are in need of a good power source that would enable them longer flight time and various functionalities. This work is focused on to this problem. A possible solution that is offered in this study is implementing a hybrid power system consisting of battery and supercapacitor (SCAP). The proposed hybrid power system was tested on an existing MAV platform (Cheerson CX-10). A separate hybrid power printed circuit board (PCB) was designed and manufactured. For experimental and system verification purposes, the PCB was not sized for on-board flight. The hybrid power PCB was connected to MAV through light power wires. To eliminate flight inconsistency, a testbed was constructed from plywood. The quadcopter was controlled using a joystick. In total, three experimental tests were conducted. In the first experiment, SCAP charge time was evaluated and compared to the calculated value. The results were very close. In the second and third experiments, MAV flight time was collected for both battery and hybrid powered MAVs for two different flight patterns. The first pattern was flying 10 seconds at low speed using battery power and 10 seconds at average speed using SCAPs power. The second pattern was flying at a fixed average speed: 10 seconds with battery and 5 seconds with SCAP power. For all the experiments, six new fully charged batteries were used. In every flight, in order to reduce the risk of decreasing battery performance, battery voltage was controlled so as not to exceed 75% depth of discharge. As soon as it reached 75% discharge rate, the flight was discontinued. At the end of the experiments, statistical data analysis was performed. The study

hypothesis that the hybrid powered MAV flight time is more than the battery powered MAV flight time was proven.

CHAPTER 1. INTRODUCTION

The purpose of this study was to increase flight time in MAVs by using battery and supercapacitor (SCAP) as a hybrid power system. As is known, the battery is still considered as the main power source in MAVs due to its flexibility in size and weight. Even though the battery satisfies size and shape parameters, it does not satisfy the performance quality of MAVs because they do not provide enough flight time. Due to this problem, in this study SCAP was proposed as an auxiliary power source. Along with the battery, it forms a hybrid power system. As shown in the Figure 1.1, SCAPs are high in specific power and low in specific energy, meaning that they can release large amounts of energy in a short amount of time.

SCAPs are known as ultracapacitors or double-layer capacitors. Their capacitance is a thousand times higher than that of an electrolytic capacitor capacitance, which is rated only in micro farads. Mostly SCAPs are used in energy storing. SCAPs are limited to 2.5-2.7 Volts. Voltages more than that can decrease their life cycle. If more than 2.7 Volts are needed, then SCAPs can be connected serially, but their total capacitance will be reduced. The specific energy of SCAPs is low (1-30Wh/kg) and the discharge rate is very high. The specific characteristics of SCAPs and a comparison to the lithium-ion battery are shown in Figure 1.2. Also, Figure 1.3 displays the advantages and disadvantages of SCAPs (*BU-210: Fuel Cell Technology*, n.d.).

One study introduced the three main characteristics of SCAPs that are important for hybrid vehicle applications: frequency, voltage, and temperature. The efficiency of SCAPs depends on these three characteristics, which can be measured by using electrochemical impedance spectroscopy (EIS). The BCAP0010 SCAP (2600F, 2.5V, temperature -20-60) from Maxwell Technologies was used in the experiment. From the experiment and measurements, it was concluded that the

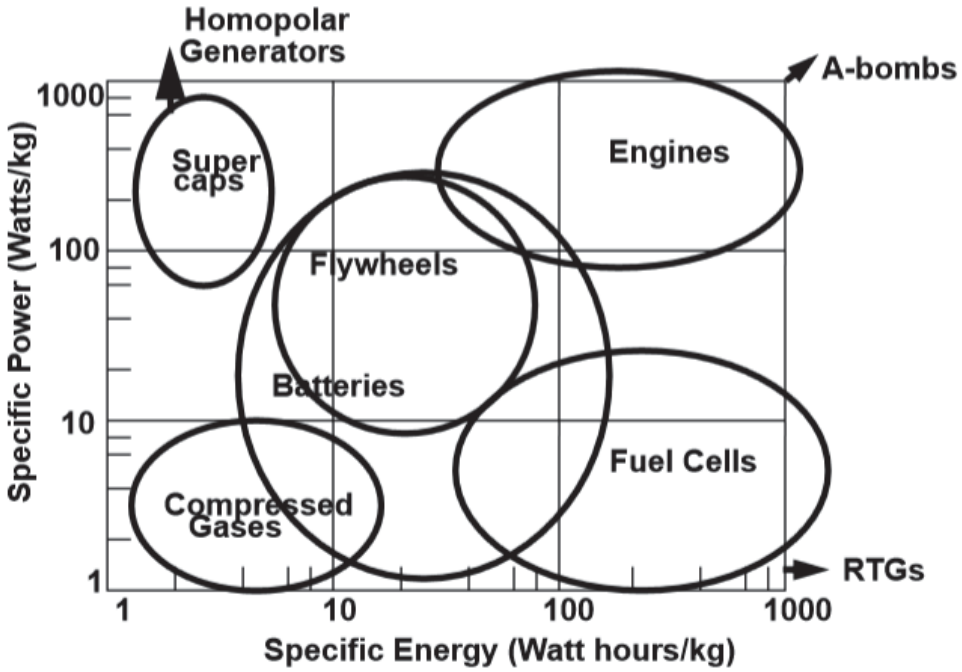

Figure 1.1. A general comparison of different technologies

(Dowling, 1997)

capacitance of SCAPs is strongly dependent on frequency. At 10Hz they can lose 90% of their capacitance. Also, at low temperatures their resistance can go up (Rafik, Gualous, Gallay, Crausaz, & Berthon, 2006).

Batteries, in comparison to SCAPs, have higher energy density and internal resistance (Figure 1.4).

Batteries are able to provide constant energy for a longer time. They do not need time for warm up, and they can start supplying energy in a couple of seconds. Rechargeable batteries have more power bandwidth but they have short service time. Batteries do not function well in below freezing temperatures because low temperatures slow down the chemical reactions inside the batteries. Batteries take a long time to recharge, which is their main disadvantage (*BU-210: Fuel Cell*

Function	Supercapacitor	Lithium-ion (general)
Charge time	1–10 seconds	10–60 minutes
Cycle life	1 million or 30,000h	500 and higher
Cell voltage	2.3 to 2.75V	3.6 to 3.7V
Specific energy (Wh/kg)	5 (typical)	100–200
Specific power (W/kg)	Up to 10,000	1,000 to 3,000
Cost per Wh	$20 (typical)	$0.50-$1.00 (large system)
Service life (in vehicle)	10 to 15 years	5 to 10 years
Charge temperature	–40 to 65°C (–40 to 149°F)	0 to 45°C (32°to 113°F)
Discharge temperature	–40 to 65°C (–40 to 149°F)	–20 to 60°C (–4 to 140°F)

Figure 1.2. SCAP and Li-ion performance comparison

(*BU-210: Fuel Cell Technology*, n.d.)

Advantages	Virtually unlimited cycle life; can be cycled millions of time High specific power; low resistance enables high load currents Charges in seconds; no end-of-charge termination required Simple charging; draws only what it needs; not subject to overcharge Safe; forgiving if abused Excellent low-temperature charge and discharge performance
Limitations	Low specific energy; holds a fraction of a regular battery Linear discharge voltage prevents using the full energy spectrum High self-discharge; higher than most batteries Low cell voltage; requires serial connections with voltage balancing High cost per watt

Figure 1.3. Advantages and limitations of SCAP

(*BU-210: Fuel Cell Technology*, n.d.)

Chemistry	Nominal voltage	Min Voltage	Max Voltage	Typical internal resistance
PbA	2.1	1.6	2.75	2-30 mΩ
NiMH	1.2	1	1.5	0.1-3 mΩ
Li-ion	3.8	2	4	2-50 mΩ
UC	1.75	0.5	3	0.02-0.2 mΩ

Figure 1.4. Electrical properties of batteries and SCAPs

(Lukic, Wirasingha, Rodriguez, Cao, & Emadi, 2006)

Technology, n.d.). There are many types of batteries depending on their chemical compositions. Figure 1.5 presents the physical properties of some of them.

Type	Energy Density Wh/kg	Power Density W/kg	Self-discharge/ month	Cycles to 80%
Pb-acid	30-45	200	5%	200-1000
Ni-Cd	40-50	190	15%	500-1000
NiMH	50-60	180	25%	500-1000
Li+	130	800	5%	1200
Ag-Zn	140-200	100-330	4%	100-250
Ag-Cd	55-95	100-220	4%	300-500
Zn-Air	200-300	80-100		N/A
Al-Air	350	500-600		N/A

Figure 1.5. Battery comparison chart

(Dowling, 1997)

Dowling (1997) in his book discusses power sources for small robots. When explaining hybrid power sources, the author notes that a hybrid power source is good at supplying small amounts of energy for a long time, but it is not good at supplying high energy for a short time. For this reason, it is suggested to have two stages of hybrid power systems. One is for high power supply and the other is for low power supply (Figure 1.6):

> ...hybrid power source can be shown in the Ragone diagram by connecting two technologies by a locus of points which provide energy and power maxima. A point along that locus can be selected to provide a specific energy greater than the less energy dense technology can achieve, source A in this case. The hybrid is a linear combination of the two technologies and thus forms a curve in log-log space (Dowling, 1997, p.10).

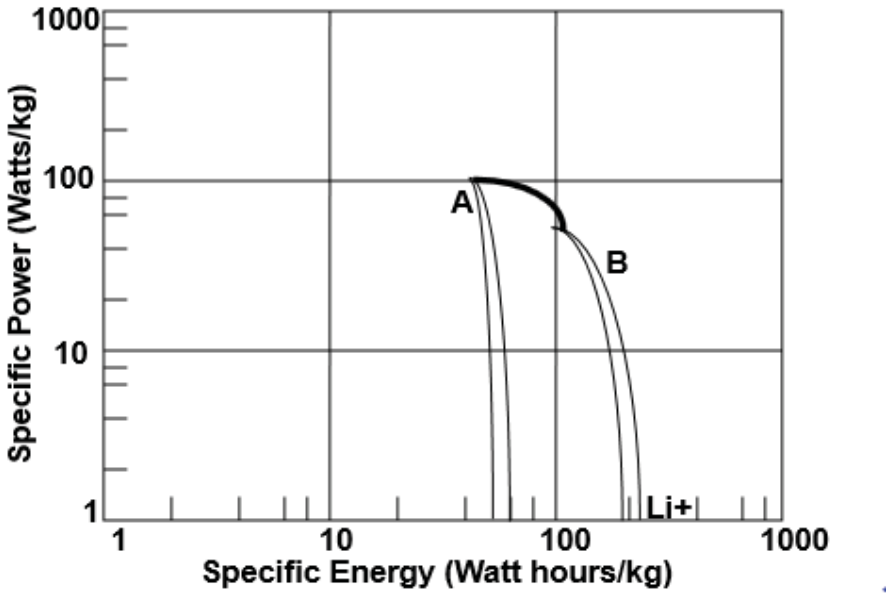

Figure 1.6. Hybrids can bridge the capabilities of different technologies (Dowling, 1997)

1.1 Motivation

The motivation to make a hybrid power system for MAVs came from an AFRL (Air Force Research Laboratory) project - Flapping Wing Robot (Figure 1.7), which is currently being researched in the M2M (Machine to Machine) laboratory.

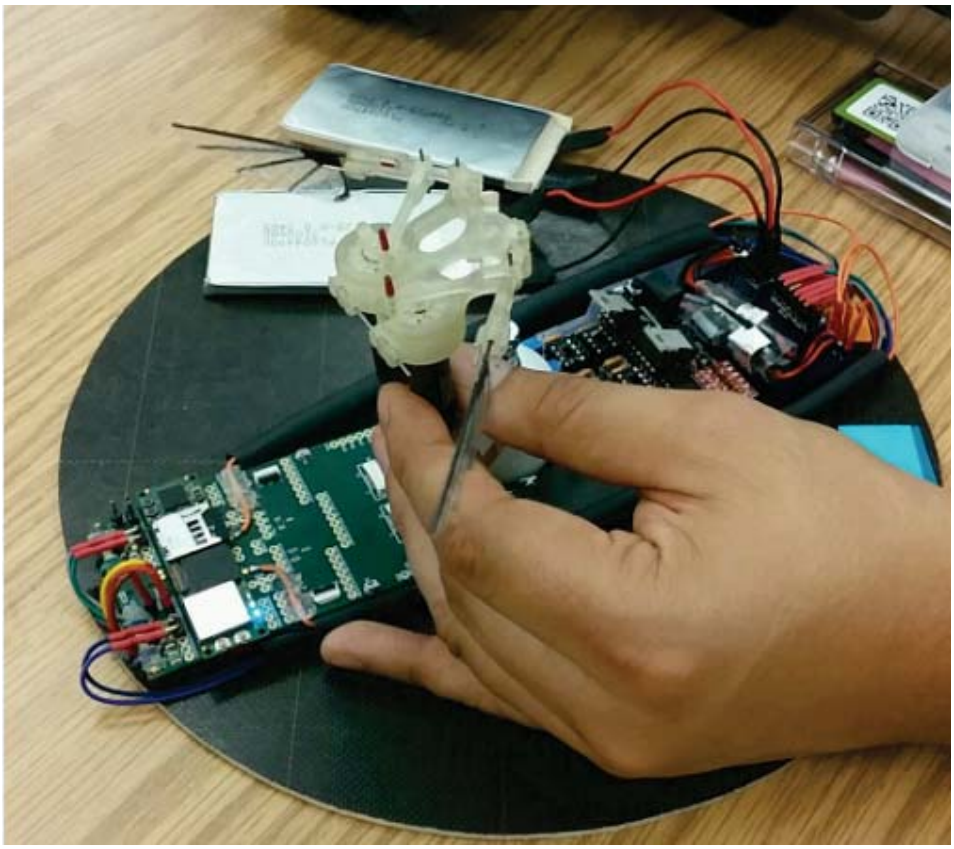

Figure 1.7. AFRL project - Flapping Wing Robot

The main purpose of this project is to build a flapping wing robot and develop model checking techniques for it. As can be seen in Figure 1.7, the flapping wing robot has been built and several model checking techniques were tested on it (Gallagher, Matson, & Greenwood, 2014; Goppert et al., 2014; Goppert, Matson, & Hwang, 2015). There is much that has been done on cyber-physical systems and adaptive hardware components of the MAV (Boddhu, Botha, McCurdy, Gallagher, & Matson, 2014; Gallagher, Matson, & Greenwood, 2013; Greenwood, Gallagher, &

Matson, 2015). A little work has been done on the MAV power management system (Perseghetti et al., 2015), where energy efficiency was improved through efficient use of internal components and flight pattern modifications. The research on the MAV is still continuing. As of today, it cannot lift itself and fly, even though it can flap its wings. A special vibration table was fabricated to test model checking techniques on the MAV. The table allows the MAV to move with its base hardware. The hardware of the MAV is not compact and is not light, which is one of the main reasons preventing MAVs from lifting themselves and flying. The power supply for such small robots remains a big problem. The 60 mg Harvard flapping wing MAV also cannot fly independently. The power is delivered to it through power wires (Wood, 2007).

The work on this area led to the proposed research question. In this study a hybrid power system will be designed and tested. A successful outcome of this study will enable the possible implementation of the system in other MAVs, in particular in the Flapping Wing MAV.

1.2 Scope

The scope of the proposed research was to investigate, determine, create, and test a hybrid power system for Micro Air Vehicles (MAVs) consisting of a battery and SCAP that increases the flight time of MAVs. To accomplish this work, a thorough power management analysis was done and implementation methods were investigated. The designed hybrid power system was tested on an existing MAV platform Cheerson CX-10 (Figure 1.8).

A separate PCB control board was designed and made for this vehicle that is able to control the hybrid power system. A micro SD card was installed on the MAV that collected all the flight data. Each test was conducted in two stages. First, the battery powered MAV flight time was collected with no platform modifications. Second, corresponding data was collected from the hybrid power

Figure 1.8. Cheerson CX-10

system (modified platform). At the end of the study, flight time results were compared. Achieving even a small amount of efficiency of the hybrid power system in this study was considered to be a success.

1.3 Significance

MAVs have six-degrees-of-freedom, which allow them to carry and use micro payloads and perform a wide range of activities. MAVs have many applications. They can be used in military situations performing rescue, tagging, and targeting. Also, MAVs can be used in fire situations, in detecting traffic, in photography, etc. The robots should be powerful enough to be able to fly long distances in order to accomplish these tasks. And here the power problem is evident. Generally, MAVs

must weigh 50 grams. Powerful conventional batteries weigh more than that. Today, small batteries are used in MAVs, but when the battery size decreases, its power decreases too. Small batteries are not power efficient.

This is why the robots cannot accomplish bigger tasks and this problem is the reason for the proposed research on hybrid power system for MAVs. Many researchers have investigated hybrid power systems. All the research was taken into consideration during this study.

1.4 Research Question

Can a battery and supercapacitor hybrid power system increase flight time in Micro Air Vehicles (MAVs)?

1.5 Assumptions

The assumptions for this study included:

- A purchased MAV was a good development platform for the research.
- An additional power control PCB (Printed Circuit Board) was wisely designed and calibrated.
- Flight measurements were taken from the onboard micro SD card. Other optimal data collection methods were investigated.
- All safety precautions were followed during experiments.
- Resulting measurement data was sufficient to confirm the hypothesis of the research.

1.6 Limitations

The limitations for this study included:

- The research focused only on power systems of MAVs.
- Measurements and results were on MAVs flight time only.
- The proposed hybrid power system can be tested in any MAV.
- When drawing conclusions, before/after weights of MAV were taken into consideration.

1.7 Delimitations

The delimitations for this study included:

- The research did not investigate and test aerodynamics, kinematics, and wing models of MAVs.
- The MAV was not built from scratch. An existing MAV platform on the market was acquired for experiments.
- It was not the purpose of the study to keep MAV weight constant during the experiments. The total weight of MAV at the end of the project could vary from its previous weight due to the additional power components.

1.8 Summary

This chapter provided a brief information about batteries and SCAPs, scope, significance, research question, assumptions, limitations, delimitations, and other background information for the research project. The next chapter provides a review of the literature relevant to the proposed thesis.

CHAPTER 2. REVIEW OF RELEVANT LITERATURE

This chapter covers important relevant previous works that have been done in the field of hybrid power systems. Also, it introduces already existing battery and supercapacitor hybrid power system management methods.

2.1 Hybrid Power Systems for MAVs

There are several studies that have been done specifically on hybrid power systems for MAVs (Micro Air Vehicles). One of the studies designed a hybrid electric motor, where potentials of a quadrotor helicopter and a gliding aircraft were combined. The method was tested on a MAV called Sharky. The design was distinctive with its ability to do a steady and free launch, to switch from glider to quadrotor and from quadrotor to glider, and to fly with support of motors. The center of mass of the MAV shifted insignificantly, providing it a better balance in gliding/motor gliding regimes. An unbalanced center of mass allows the MAV to use generated potential energy for transitions and rotations. When the robot is in the gliding regime, it decreases the use of the brushless motor, which is very advantageous for minimization of battery usage. The design enables the robot six degrees of freedom if the angular velocity of the motors is properly configured. The whole mechanical structure of the MAV was made from carbon fiber, which decreases vibration during the flight. The MAV was tested in a wind tunnel and the results were recorded. The test gave a small pitching number, which leads to the conclusion that the proposed method requires less motor and battery power. The researchers concluded that the experimental results needed further improvements and thorough analysis (Sampaio et al., 2014).

Another hybrid power system that was proposed is a combination of Direct Methanol Fuel Cell (DMFC) and battery. The main goal was to combine the outputs of both power sources into one output that will satisfy the requirements of MAV avionics. The SDCOC (Stochastic Drift Counteraction Optimal Control) approach was used in this research. This is a power dividing control method that balances power between the fuel cell and battery and increases the flight time of MAV. Fuel cell and battery models and schematics were made that combine both powers together. The fuel cell was highly efficient when the robot had a low climb angle and low propeller power. At this fuel state, it charged the battery. This method indeed maximized the flight time and decreased failures during flights (Balasubramanian, Kolmanovsky, & Saha, 2012).

It is very difficult to replicate exact insect wing kinematics because insects have a very complex wing structure. Insect robots, without using tail motion, have to perform asymmetric wing motions. Therefore, asymmetrical wing control kinematics is required. The solution of using two different actuators, a bigger power actuator and smaller control actuator, was proposed to solve this problem. The research subject was the Harvard Microrobotic Fly, which previously had one degree of freedom symmetrical power actuator that only allowed pitch. In this paper, two small control actuators were added to the fly allowing it to generate asymmetry and yaw torques. Also, two tiny pieces of a Reflexite tape were put on the edges of the wings to increase the inertia. Measurements were made at 20-40 Hz frequency and at a constant amplitude. To capture the flight of the MAV, a high speed video recording device was used. According to the results of the experiment, the actuators generated higher torque and higher power for flapping wings. The researchers are aiming to build a better structural design and a better control method in the future (Finio, Eum, Oland, & Wood, 2009).

The conventional lead acid battery that is used in mobile robots was replaced with the PEM (polymer electrolyte membrane) fuel cell. Conventional batteries need 10 hours and PEMs need 15 minutes to refill. There are a wide variety of PEM

fuel cells on the market. The researchers chose a 10W stack fuel cell due to its ability to work with air instead of pressurized oxygen. Also, this fuel cell was able to supply 10V, 2A, 10mW/cm^2 at no load state. Even though fuel cell selection was not difficult, hydrogen storage was a problem. Small storage tanks were relatively heavy for this application. Despite this, a small tank with a volume of 20 liters was chosen. A pressure regulator was used to control hydrogen flow pressure at 3psi. However, the hydride tank worked only at 7 psi. To remove excess hydrogen, a purging algorithm was programmed in a microcontroller. The algorithm controlled the current and voltage of the fuel cell, and when the electrical values fell below the curve in Figure 2.1, the microcontroller activated a small solenoid valve that blew

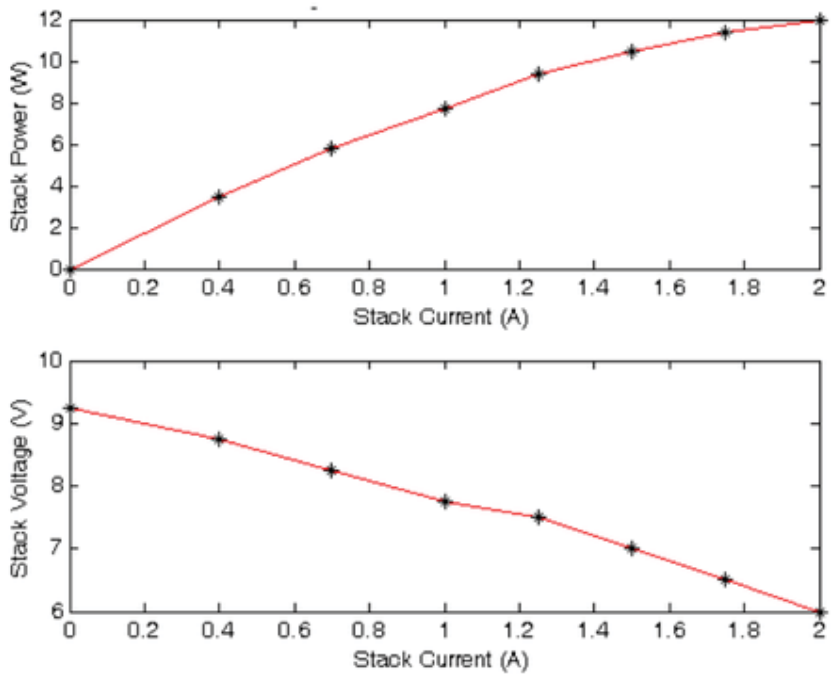

Figure 2.1. Characteristic curves of selected fuel cell

(Wilhelm, Surgenor, & Pharoah, 2005)

away the excess hydrogen. To regulate the power supply to 12V, LM2588 DC/DC converter circuit was used. As a result of the experiment, the mobile robot ran two

hours with a full tank. According to the authors, the results were not as good as expected due to the small size of the fuel tank, which limited the power supply (Wilhelm et al., 2005).

2.2 Hybrid Power Systems for Electric Vehicles

A combination of battery and SCAP in a hybrid electric vehicle is a broader topic than its implementation in MAVs. Here is one example of a hybrid electric car using those two power sources. In the research ZEBRA (sodium-nickel-chloride), the battery was chosen due to its high energy density, almost no self-discharge, high energy efficiency, and low cost. The battery was the primary power source and SCUP was an additional power source. In order to match SCUP and battery voltages, a DC/DC converter was used. When designing the converter, all the power losses were taken into consideration, which included the inductor, capacitor, diode, power silicon, turn-off, and conduction losses. The results of the simulations revealed that the combination of battery and SCAP improved the voltage fluctuation and decreased the power loss (Jarushi & Schofield, 2010).

Another hybrid method was designed for the electric vehicle. Connection between the battery and the SCAP was established using two half-bridge DC/DC converters. This allowed control of the powering flow more efficiently. Two control strategies were investigated: power flow management strategy, which increases power efficiency, and SCAP management strategy, which increases battery life by eliminating excess current stress on the battery. The first strategy gave a 7.6% improvement, and the second strategy gave a 72% improvement. However, it was not possible to implement both strategies at the same time. One strategy take priority over the other (Carter & Cruden, 2008).

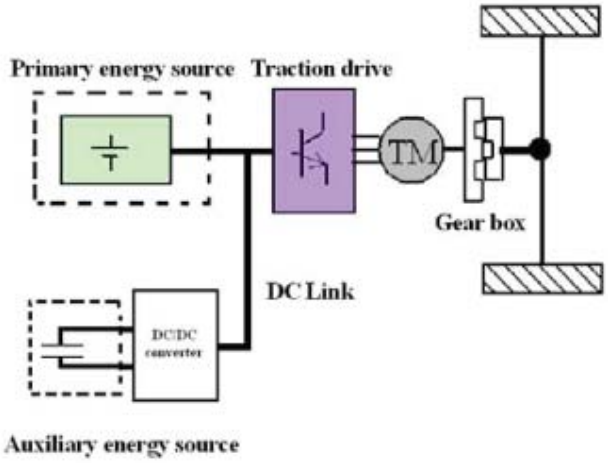

Figure 2.2. Hybrid energy source in electric vehicles

(Jarushi & Schofield, 2010)

2.3 Hybrid of Battery and SCAP

A combination of battery and SCAP has been studied and a number of papers were published on this. Every paper has unique experimental methods for implementing this system. Some of the research will be further elaborated and the methods explained.

2.3.1 Parallel and Serial Connection of the Sources

As was described in the book of Dowling, two power sources can be connected in serial and in parallel. A serial design provides low energy at the first stage and high energy at the second stage. On the other hand, a parallel design can provide either (low, high) energy at any time. This is why the parallel method is used in many hybrid vehicles (Dowling, 1997).

2.3.2 Passive Parallel Method

In this method, the battery and SCAP are connected directly parallel without any power converters (Figure 2.3). For this reason, all the voltages are equal. SCUP here acts as a low pass filter. The advantages of such a configuration are simplicity and cost efficiency. The disadvantage of the configuration is that SCAP energy cannot be used efficiently (Cao & Emadi, 2012; Lukic et al., 2006).

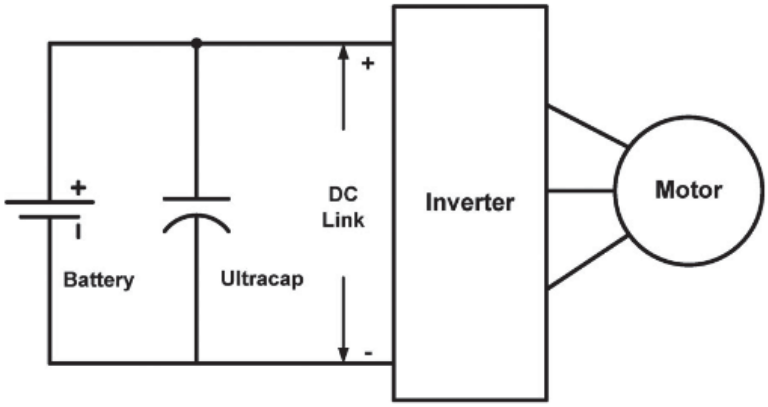

Figure 2.3. Passive parallel configuration

(Cao & Emadi, 2012)

2.3.3 Active Parallel Methods

Active parallel methods use one or more power converters. There are several studies where active parallel methods were implemented.

In one study, researchers connected the two power sources in parallel to reach a better performance. The proposed method used a DC/DC converter where a SCAP should be charged at buck cycle and discharged at boost cycle. Thus, energy flow was regulated with a pulse-with-modulated (PMW) DC/DC converter.

The experiment concluded that when using a DC/DC power converter:

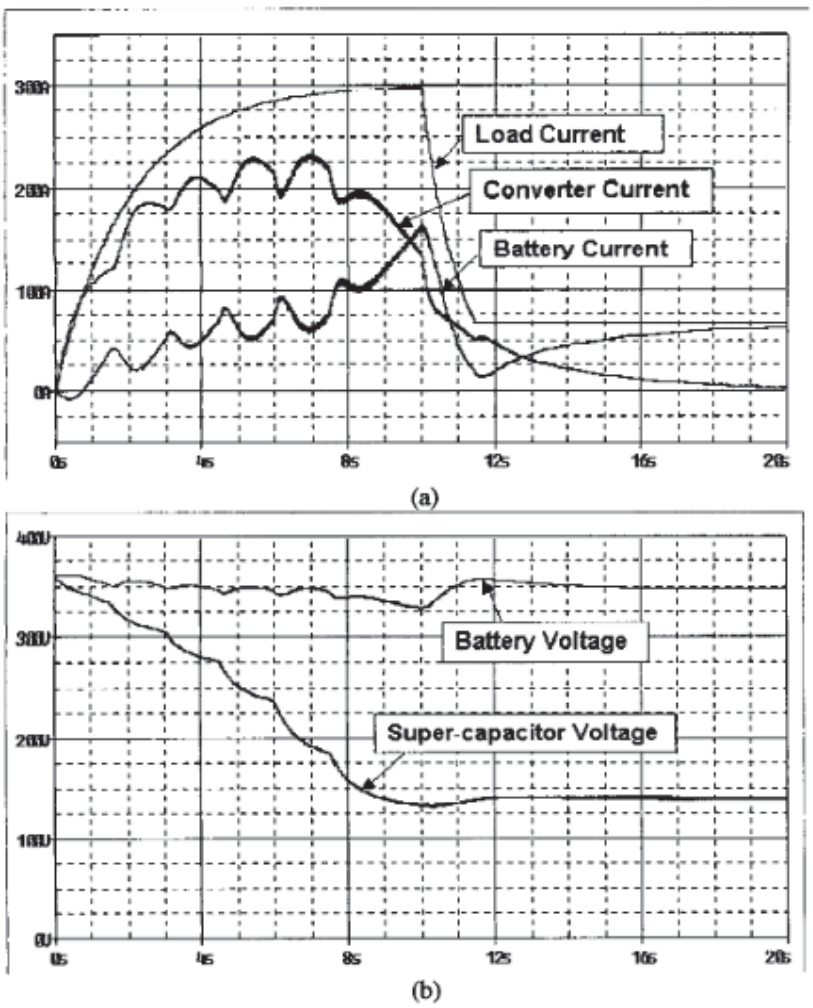

Figure 2.4. Battery and SCAP simulation with power converter: a) currents b) voltages during acceleration

(Pay & Baghzouz, 2003)

- Peak current of battery decreases by 40%
- DC voltage control improves by 30%
- State of charge of the SCAP becomes 3.5 times higher ...

The study made the conclusion that parallel connection of a battery and a SCAP and implementation of a DC/DC power control circuit decreases stress on

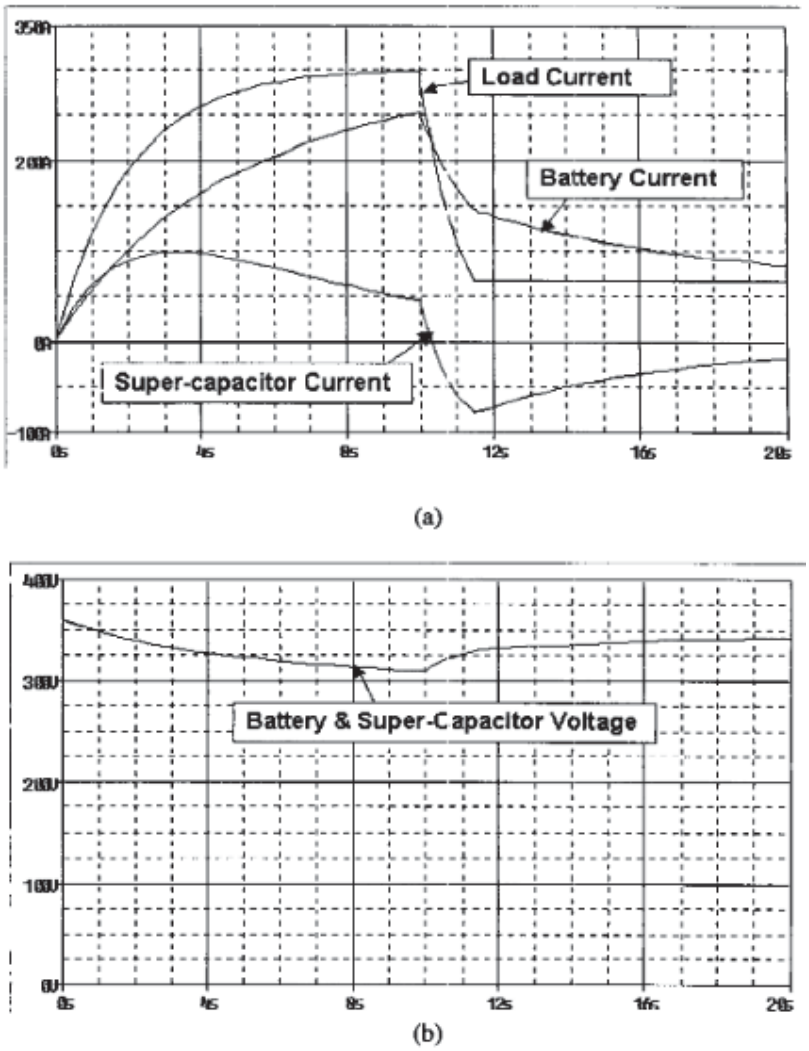

Figure 2.5. Battery and SCAP simulation without power converter: a) currents b) voltages during acceleration

(Pay & Baghzouz, 2003)

the battery and allows the use of all the capabilities of a SCAP. The study results can be observed from Figure 2.4 and Figure 2.5 (Pay & Baghzouz, 2003).

Another study claimed that the hybrid of a battery and a SCAP can reach more specific power by decreasing battery current and stress. Also, it is believed that this hybrid will provide longer run-time. Connecting these power sources

directly in parallel prevents controlling the terminal voltage of the hybrid system. It will just follow a battery discharge chart. The researchers in this paper worked on an improvement of the hybrid system by using a DC/DC converter (Figure 2.6). As a result, they figured out that an actively controlled hybrid system can improve the power rate up to three times. In addition, this hybrid system has these advantages: wide voltage range, better voltage regulation, fewer current fluctuations, and light weight of the system in general. Also, the DC/DC converter can serve as a battery charging unit. A battery-only system has these advantages: higher power peak, longer battery lifetime, and higher efficiency. But when it is directly combined with a SCAP these advantages change. The load voltage, SCAP voltage, and battery voltage ramble together, limiting a full exploration of SCAP advantages.

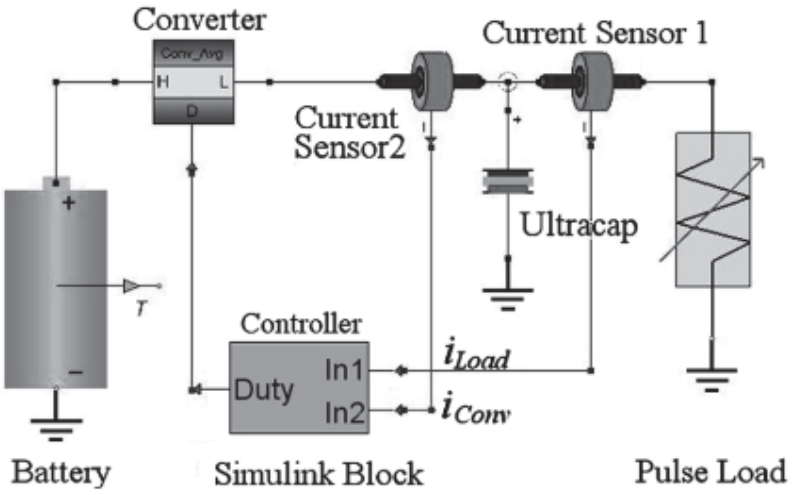

Figure 2.6. Active hybrid connection

(Gao, Dougal, & Liu, 2005)

The working principle of the DC/DC converter controlled hybrid system is that when the load has a small current, the battery constantly charges and discharges the SCAP. Discharge rate depends on the load requirements and is controlled via a special feedback system. To keep the battery at a safe condition, its

current was controlled to keep it at a safe mode. The charging current was higher than the battery current and it was identified through a duty ratio. When the load needed more current, both power sources supplied the current, but the battery current stayed at the same constant level and the rest of the current was supplied by the SCAP. Keeping the battery current at the steady level provided safety and long life for the hybrid system. At the same time, it provided higher power with no excessive stress on the battery (Gao et al., 2005).

An active hybrid method for an energy storing system was investigated in another research paper (Zhang, Jiang, & Yu, 2008). The system consisted of a main power source, a battery, and a SCAP. Putting DC/DC converters between each power source allows efficient control of the system. In this design, the main power source supplies average load power, and the battery and SCAP supply peak and transient powers. Because the SCAP discharges very fast, the battery helps to recover by supplying some power to it. Three control methods were used in this system:

1. When the load demand is high, the first battery discharges until the current reaches ib1 threshold. After this, the SCAP starts discharging. But if the load demand is low, both the battery and SCAP charge.

2. When the load requires high power, both the battery and SCAP discharge together. And when the load requires low power, the battery charges first until the current reaches another ib2 threshold. When the threshold is reached, SCAP joins the charging state.

3. The battery discharges first, and later the SCAP, when the battery current reaches ib1 threshold.

Conclusions from the experiment and simulations:

- In the first method, the battery uses more power, while the SCAP has the most power.

- In the second and third method, the battery has the most power, while SCAP uses more power. It is important to choose the right controller parameters in order to achieve the best hybrid storage system performance (Zhang et al., 2008).

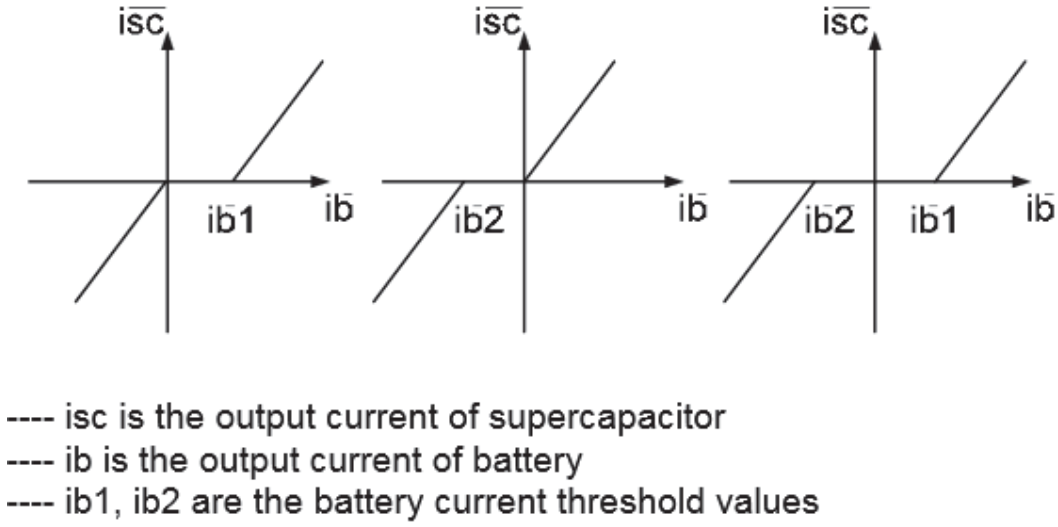

Figure 2.7. Battery and SCAP control strategies

(Zhang et al., 2008)

Later in this subsection, different configurations of the active parallel method will be presented.

2.3.3.1. SCAP/Battery Configuration

In this configuration, the SCAP comes before the battery. The configuration uses a bi-directional DC/DC converter to control the SCAP voltage (Figure 2.8). The size of the converter should be large enough to handle the SCAP power. DC link voltage stays the same due to its direct connection to the battery (Camara,

Gualous, Gustin, Berthon, & Dakyo, 2010; Cao & Emadi, 2012; Ortúzar, Moreno, & Dixon, 2007).

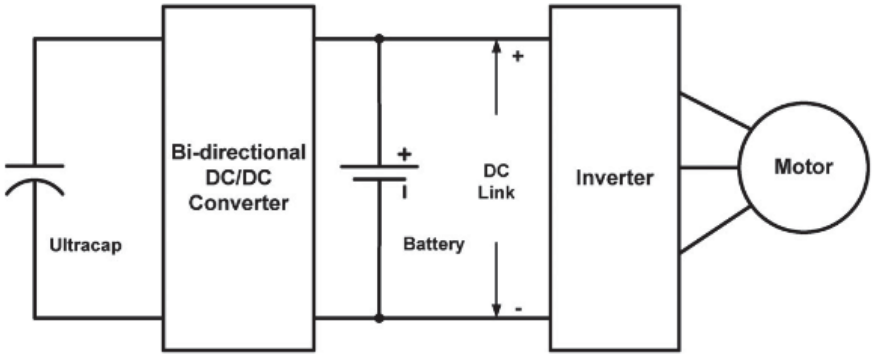

Figure 2.8. SCAP/Battery configuration

(Cao & Emadi, 2012)

2.3.3.2. Battery/SCAP Configuration

In this configuration, the battery comes before the SCAP. They are divided by a bi-directional DC/DC converter (Figure 2.9). The battery voltage can be less or more than the the SCAP voltage. DC link voltage can vary in a range that enables efficient usage of SCAP power because it is directly connected to the SCAP. SCAP here acts as a low pass filter (Cao & Emadi, 2012).

2.3.3.3. Cascaded Configuration

This configuration uses two bi-directional DC/DC converters after each power source (Figure 2.10). It is an improved version of the battery/SCAP configuration that allows better SCAP work (Cao & Emadi, 2012).

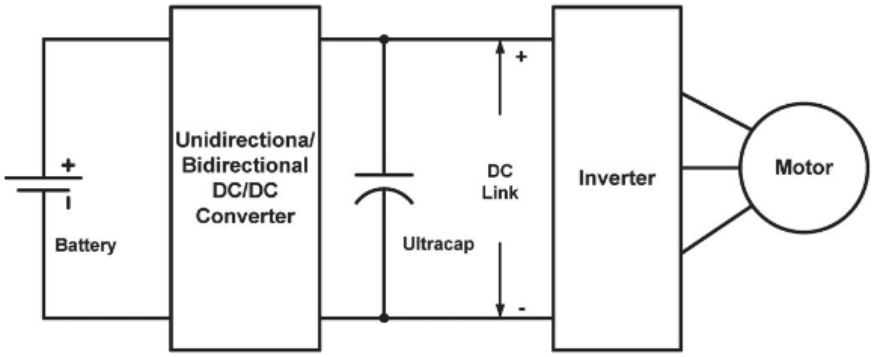

Figure 2.9. Battery/SCAP configuration

(Cao & Emadi, 2012)

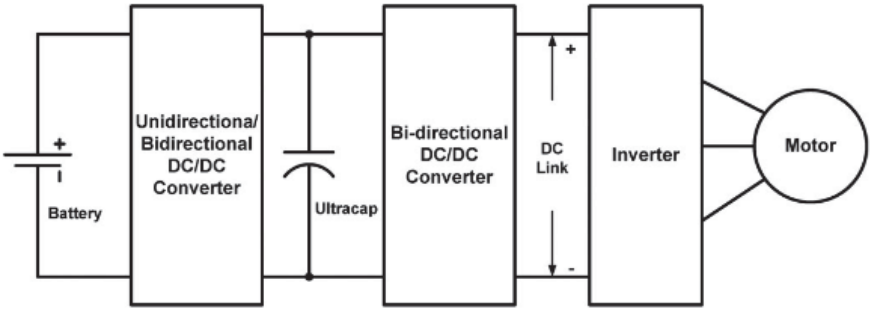

Figure 2.10. Cascaded configuration

(Cao & Emadi, 2012)

2.3.3.4. Multiple Converter Configuration

In this configuration, each power source is independently connected to a bi-directional converter and gives parallel outputs (Figure 2.11). The parallel output voltages are equal to the DC link voltage. This eases the voltage balancing issue. The configuration needs two converters, which is the drawback of the system (Cao & Emadi, 2012).

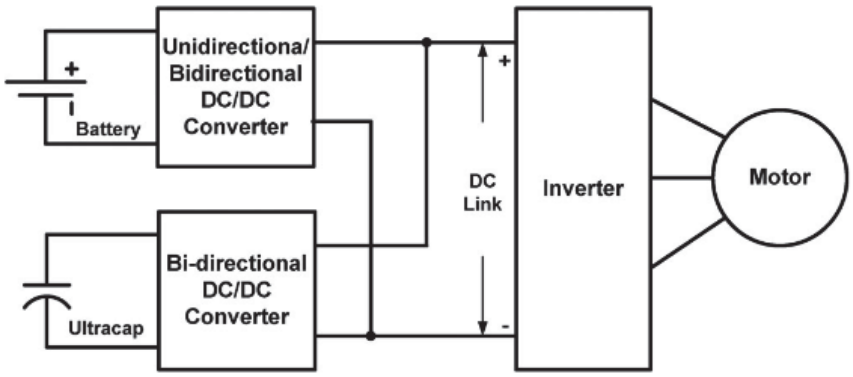

Figure 2.11. Multiple converter configuration

(Cao & Emadi, 2012)

2.3.3.5. Multiple Input Converter Configuration

As was seen from the multiple converter configuration, using multiple full size converters is not cost efficient. Instead of using many converters, a single converter with multiple inputs can be used (Cao & Emadi, 2012; Di Napoli, Crescimbini, Guilii Capponi, & Solero, 2002). The schematic of the configuration is shown in Figure 2.12.

2.3.3.6. Battery/SCAP Configuration with Smaller Converter

The study proposed to use a small DC/DC converter instead of a large DC/DC converter (Figure 2.13). The high voltage SCAP is directly connected to DC link, and the low voltage battery is connected to the DC link through a power control diode. The small size converter is placed between the power sources and constantly supplies power to the SCUP. When SCAP voltage drops to a very low value, the battery instantly supplies voltage to it. Therefore, a balanced constant power is provided to the load.

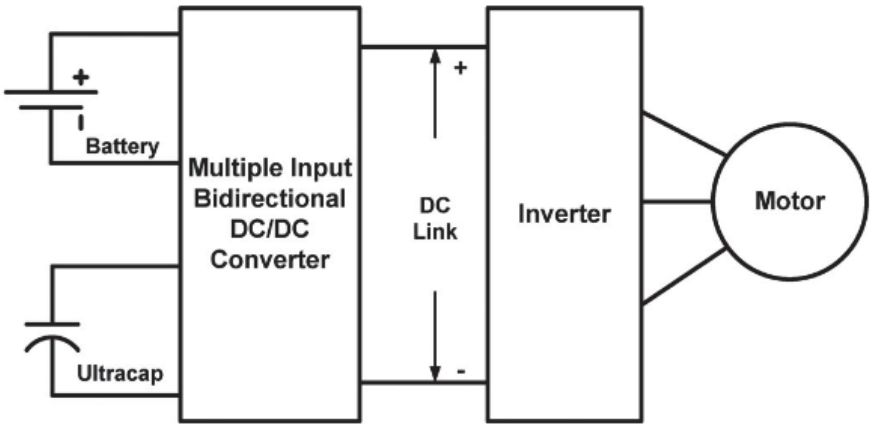

Figure 2.12. Multiple input converter configuration

(Cao & Emadi, 2012)

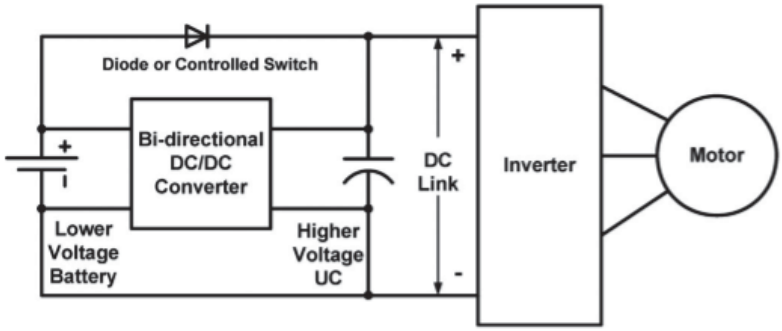

Figure 2.13. Hybrid system with smaller size DC/DC converter

(Cao & Emadi, 2012)

During the creation of the model voltage regulation, size, cost, safety, and reliability characteristics were taken into consideration. Moreover, four operating modes of the design were analyzed. It is believed that this design increases battery life, and it is cost efficient (Cao & Emadi, 2012; Khaligh & Li, 2010).

2.3.3.7. Double Inverter Method

Using a double inverter in the hybrid of the battery and SCAP instead of heavy, high loss, and high cost DC/DC converters was supported by another study. Two level and three level inverters were used in the system (Figure 2.14). A battery and a SCAP were connected to the three level diode connected inverters. This circuit organization increases power efficiency and eliminates the need for DC/DC converters (Vilathgamuwa, Jayasinghe, Lee, & Madawala, 2011).

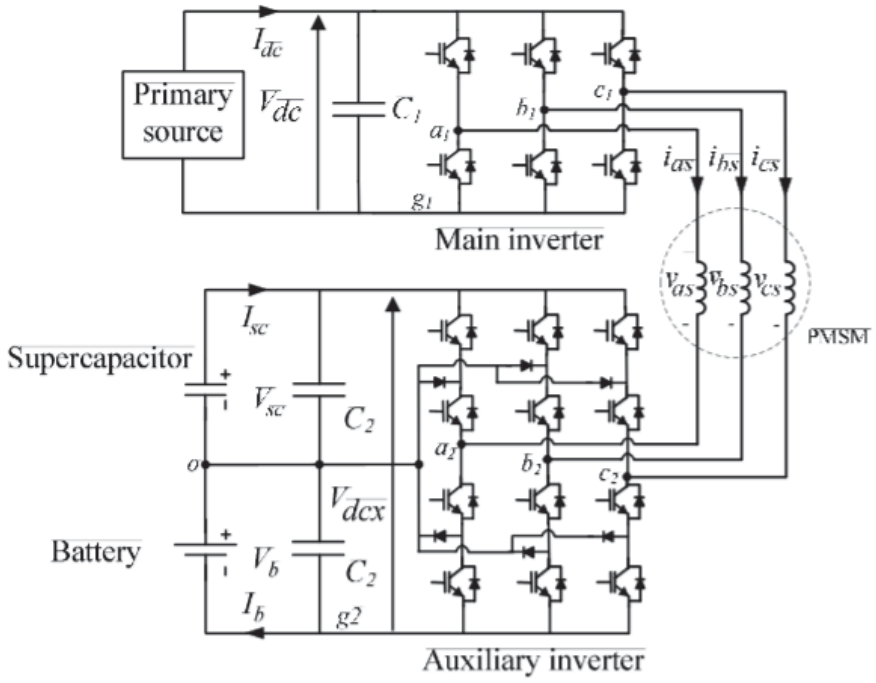

Figure 2.14. Double inverter method

(Vilathgamuwa et al., 2011)

2.4 Summary

This chapter provided a review of the literature relevant to the proposed research question. Relevant implementation methods for the battery and SCAP were briefly discussed. The next chapter provides the framework and methodology used in this research project.

CHAPTER 3. FRAMEWORK AND METHODOLOGY

This chapter provides the framework and methodology used in the study. From the methods discussed in the previous chapter, the battery/SCUP configuration with smaller converter was chosen. As is known, the size and weight of the power system is very important for MAVs. For this reason, a smaller converter method was selected for implementation. The battery/SCAP configuration increases the efficiency of SCAP because it is directly connected to the DC link. The final PCB should have a power control circuit that uses the battery/SCUP configuration with smaller converter and an on-board micro SD card for flight data collection purposes. Later in this chapter, the detailed implementation plan will be discussed.

3.1 Proposed Hybrid Power System Design

The development platform Cheerson CX-10 was chosen for this study because of its similar characteristics to those of MAVs (light weight and small size). It is powered from a single cell 3.7V 100mAh Li-ion battery. The battery discharge rate is 2C. In order to verify that the proposed hybrid power system qualifies for this vehicle, initial simulations were done using MATLAB/Simulink tool (Grama, Patarau, Etz, & Petreus, 2014). The following circuit only checks the battery discharge rate (Figure 3.1).

From the output graph, it can be observed that the battery fully discharges in 1800 seconds.

In the next circuit, along with the battery discharge current, load current was added. For experimental purposes, 0.2A current was assigned for each of the four motors of the quadcopter. In this case, voltage ripples can be seen from the output graph, and the battery fully discharges in 440 seconds (Figure 3.2).

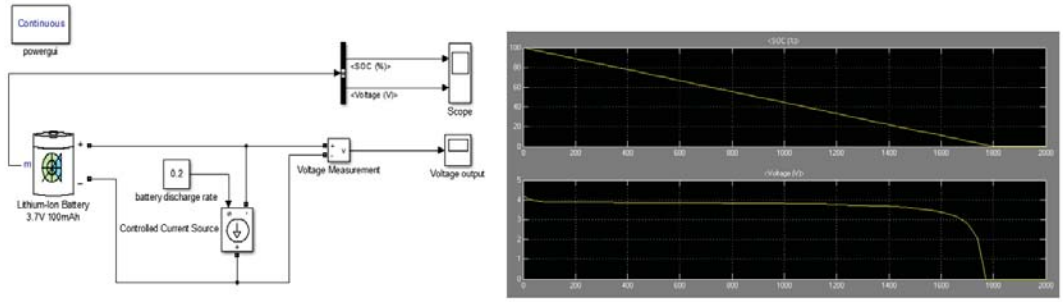

Figure 3.1. Battery discharge checking circuit

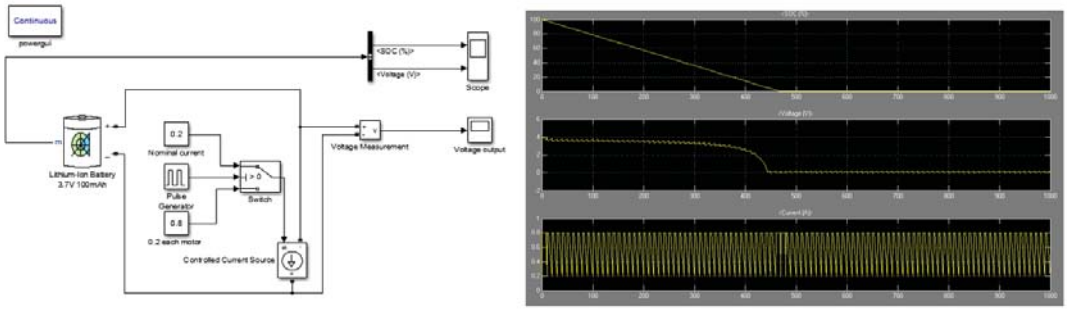

Figure 3.2. Battery discharge state when load added

In the following circuit along with the battery, a SCAP was added to the circuit (Figure 3.3). This helped to decrease the ripple amount in comparison to the previous graph.

Finally, a converter was added to the circuit (Figure 3.4). As can be observed from the output graph, there is a time difference of approximately 60 seconds between the two power systems. From all the simulations above, it can be seen that the hybrid power system consisting of a battery and a SCAP can decrease voltage variations and possibly increase battery use time. However, it should be

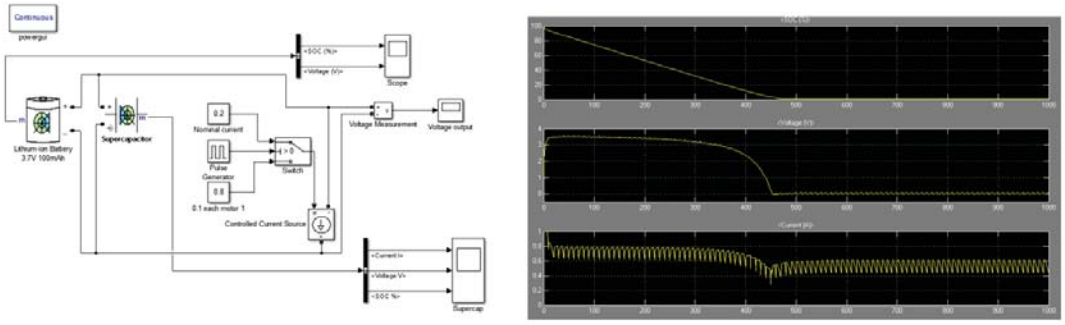

Figure 3.3. Passive hybrid power system simulation

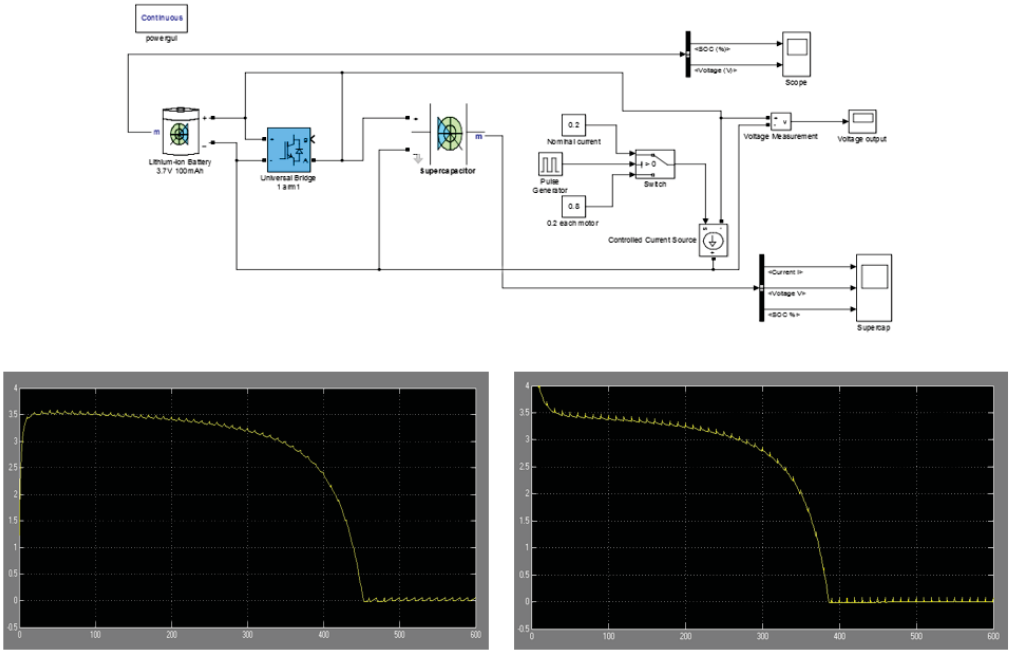

Figure 3.4. Active hybrid power system simulation

noted that the simulations do not take into account the weight of the system and its effect on the battery.

After getting a basic sense of a possible hybrid power system design, the following design in Figure 3.5 was proposed for this study.

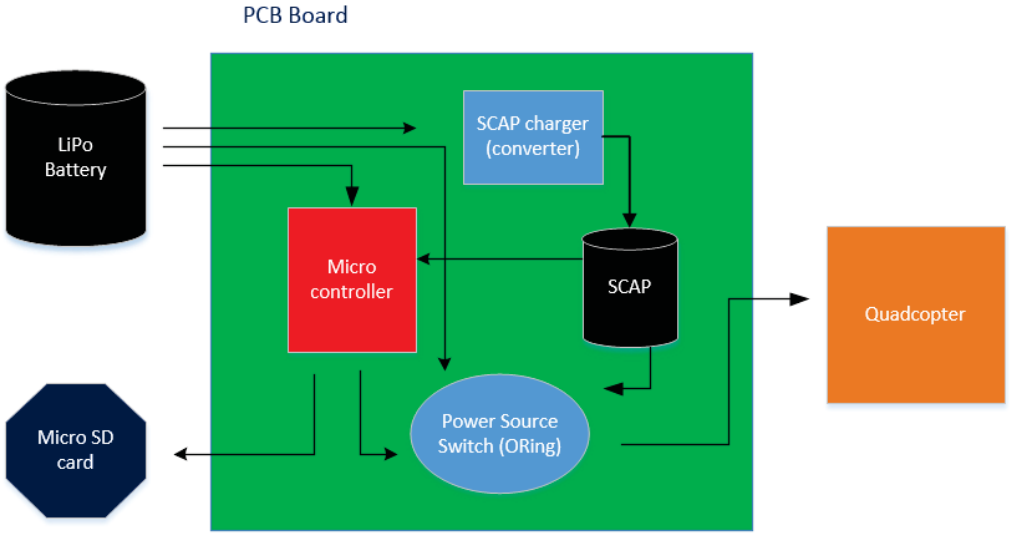

Figure 3.5. Proposed hybrid power system design

The proposed hybrid power system was designed to be a separate PCB from quadcopter's control board. The PCB controls and manages two power sources. In this design, it can be assumed that the battery is the main power source and SCAP is an auxiliary power source. Other than these two power sources, the PCB contains other components such as a SCAP charger (converter), a power switching system, and a microcontroller. Because SCAP has a high discharge rate, it has to be constantly charged. Therefore, the SCAP charger that is fed from the battery was decided to be used. A power switch was used to control two power sources because they cannot power the load at the same time. In order to visualize the changes in voltage, a micro SD card that records all the power data was implemented. The whole hybrid power system is controlled by a microcontroller. Output from this power board goes directly to the quadcopter.

In this study, for system verification purposes, the size of the system was not taken into consideration; instead the compatibility of components and the efficiency of the system were given a bigger priority. From the following system components section, one can find a better understanding about it. The system was not designed for on-board flight; instead, power wires were used to supply power to the quadcopter (Ma, Chirarattananon, Fuller, & Wood, 2013). Again, this is only for system verification purposes. After successful system tests, a smaller on-board version of the system can be produced.

3.2 Proposed System Components

3.2.1 Li-Po Battery

The Li-Po battery is a rechargeable power source (*3.7V 300mAh Li-Po battery datasheet*, n.d.). Specifications of the battery are given in Table 3.1.

Table 3.1
Li-Po battery specifications

Nominal Voltage	3.7V
Nominal Capacity	300mAh
Standard Discharge Current	0.2C
Discharge Lower Limit Voltage	3V
Standard Cycle Life	>=300 times
Weight	9.0 g
Dimensions	35 x 20 x 6 mm

This battery was chosen because it satisfies the demands of the SCAP charger. It is able to quickly supply enough power to keep SCAP charged.

3.2.2 Supercapacitor

SCAP is from the HB series of Eaton Bussmann manufacturer (*HB Supercapacitor datasheet*, n.d.). It has the advantages of low ESR (Equivalent Series Resistance), high capacitance, and light weight in comparison to other SCAPs. Detailed specifications can be found in Table 3.2. In this study, two pieces of these SCAPs were used.

Table 3.2
SCAP specifications

Item	**1 SCAP Specs**	**2 SCAP Specs**
Working Voltage	2.5V	5.0V
Capacitance	3.0F	1.5F
ESR	0.155 - 0.160 Ohms	0.31 - 0.32 Ohms
Weight	1.5 g	3.0 g

3.2.3 Supercapacitor Charger

The SCAP charger from Linear Technology is a programmable unit that is able to charge two SCAPs in series. There are two models of these chargers: LTC3225, which outputs fixed voltage of 4.8V/5.3V, and LTC3225-1, which outputs fixed voltage of 4.0V/4.5V. This charger is very suitable for small battery systems. It has an automatic cell balancing system that prevents SCAP damages. Input voltage can vary from 2.8V to 5.5V. Charge current can be programmed through external resistor and can go up to 150mA. The charger constantly charges two SCAPs in series until SCAPs reach the fixed output voltage. When the fixed output voltage is reached, the charger stops charging and starts recharging back as soon as the output voltage drops. The charger is encapsulated in a 10 lead 2x3 mm DFN

(dual-flat no-leads) package (*LTC3225/LTC3225-1 Supercapacitor charger datasheet*, n.d.). A typical schematic of the charger can be seen in Figure 3.6.

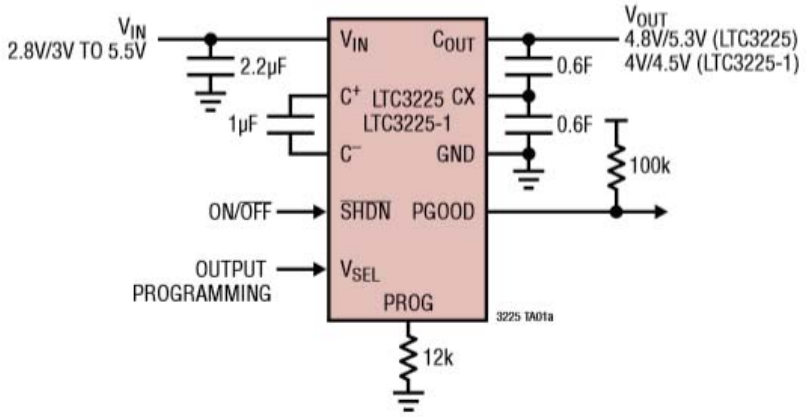

Figure 3.6. LTC3225/LTC3225-1 schematic

(*LTC3225/LTC3225-1 Supercapacitor charger datasheet*, n.d.)

For this study, the LTC3225-1 version was selected because of its fixed output voltage 4.0V/4.5V. The charger has an internal buck-boost converter that balances the output voltage to a fixed value. So, there is no need to use another converter to control the output voltage variations because the battery and SCAP output voltages are roughly balanced (3.7V and 4.0V). Input/output charge currents were calculated according to the equations provided on the charger datasheet.

$$I_{Vin} = \frac{3600V}{R_{prog}} = \frac{3600V}{12000Ohms} = 0.3A, \tag{3.1}$$

where a programmable resistor value of 12k Ohms was selected.

$$I_{out} = \frac{I_{Vin}}{2} = \frac{0.3A}{2} = 0.15A \tag{3.2}$$

Charge time can be calculated using this equation:

$$t_{charge} = \frac{C_{out}(V_{cout} - V_{ini})}{I_{out}}, \tag{3.3}$$

where C_{out} is total output capacitance from two series capacitors, V_{cout} is the output voltage threshold depending on the LTC3225/LTC3225-1 versions, V_{ini} is the initial voltage in SCAPs, and I_{out} is the output charge current.

3.2.4 Ideal Diode IC

This is an ideal diode IC that is able to supply up to 2.6A. Input voltage to the diode can vary from 2.6V to 5.5V. This compact IC is enclosed in a 5 lead 1mm SOT-23 (Small Outline Transistor) package. It is a very suitable component for small power systems due to its small size and light weight (*LTC4411 Ideal diode datasheet*, n.d.). LTC4411 was selected for this design because of its capability to control two power sources using a microcontroller (Figure 3.7).

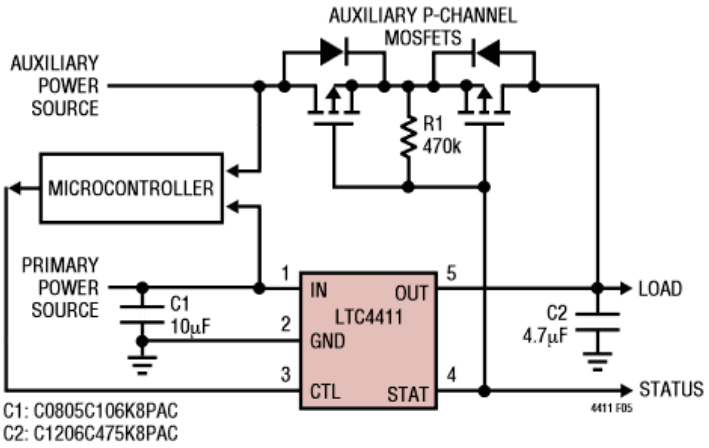

Figure 3.7. Load switchover between two power sources

(*LTC4411 Ideal diode datasheet*, n.d.)

Triggering CTL pin LOW switches the load to a primary power source, while triggering it to HIGH switches the load to an auxiliary power source which has been done with the help of back-to-back P-Channel MOSFETs.

3.2.5 Dual P-Channel MOSFET

Si1965 is a Vishay manufactured MOSFET (*Dual P-Channel MOSFET Si1965 datasheet*, n.d.). The chip incorporates two P-Channel MOSFETs, creating a dual P-Channel MOSFET. Its $R_{DS_{on}}$ value at V_{GS} = -4.5V is equal to 0.390 Ohms. The MOSFET was used in the design with LTC4411 for power source switching purposes.

3.2.6 Microcontroller ATmega328P

ATmega328P is an 8 bit microcontroller chip that is widely used in Arduino and other AVR boards (*ATmega328P microcontroller*, n.d.). It operates in 1.8-5.5V, and has 23 programmable I/O lines. In this study, ATmega328P controls LTC4411 and logs data to an SD card.

3.2.7 Micro SD Card Data Logger

OpenLog is an open source data logging system developed by Sparkfun Electronics (*Sparkfun OpenLog*, n.d.). It is a light weight and compact sized (4 x 15 x 19mm) device that is very easy to use (Figure 3.8). Once OpenLog is configured, it writes/reads data from a serial port.

3.3 Finalized System Design

After the selection of all the components for the system, they were integrated into a single system circuit design as can be seen in Figure 3.9. CadSoft EAGLE Software was used in designing the circuit and the PCB (Figure 3.10). The dimensions of the PCB are 68x46x3mm. The microcontroller on the PCB takes almost a half board space because the DIP (Dual In-line Package) version of Atmega238P was implemented. This was done intentionally so that it would be easy to take the chip off for programming and put it back. Otherwise, the TQFP

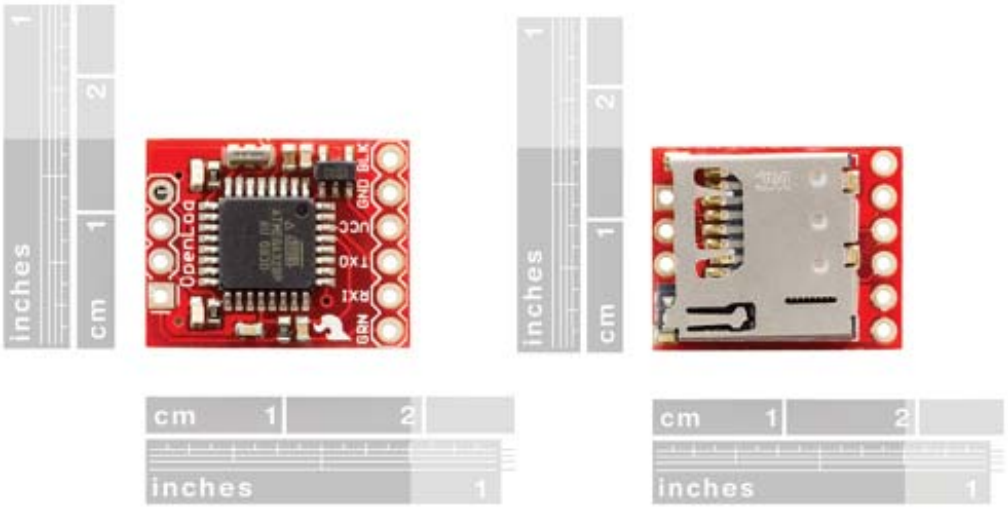

Figure 3.8. OpenLog SD card data logger

(*Sparkfun OpenLog*, n.d.)

(Thin-profile Quad Flat Pack) package of ATmega328P can be used because it does not take much space.

A completely built PCB board is displayed on the Figure 3.11. The total weight of the built PCB is 19 grams and size is 66x46x25 mm. It has slots for battery input, OpenLog SD card data logger connections, and load connections. All the external connections were done via jumper wires (Figure 3.12).

3.4 Summary

This chapter provides the framework and methodology that was used in the research study. The next chapter provides the experimental results.

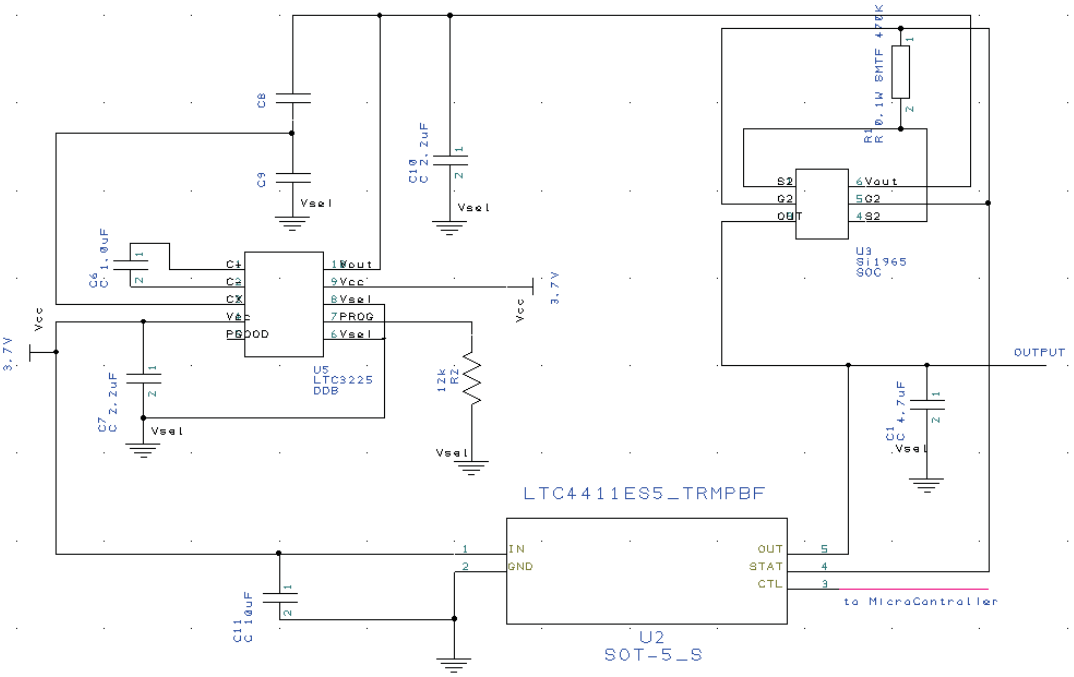

Figure 3.9. Hybrid system circuit

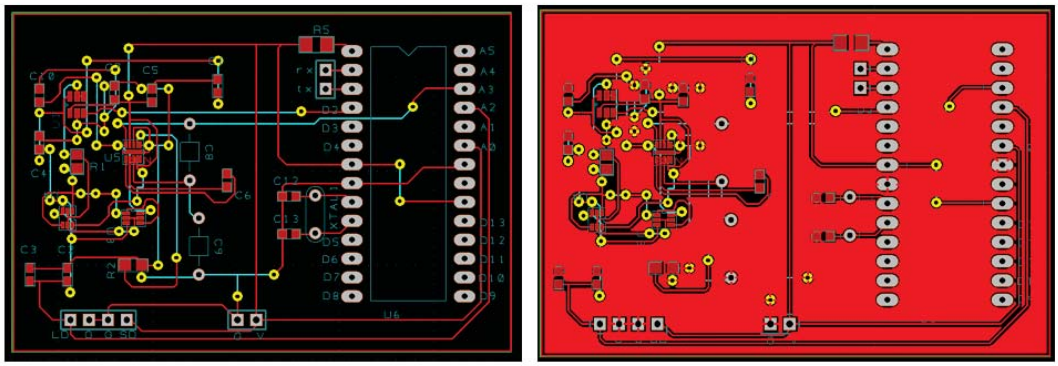

Figure 3.10. Hybrid system PCB layout

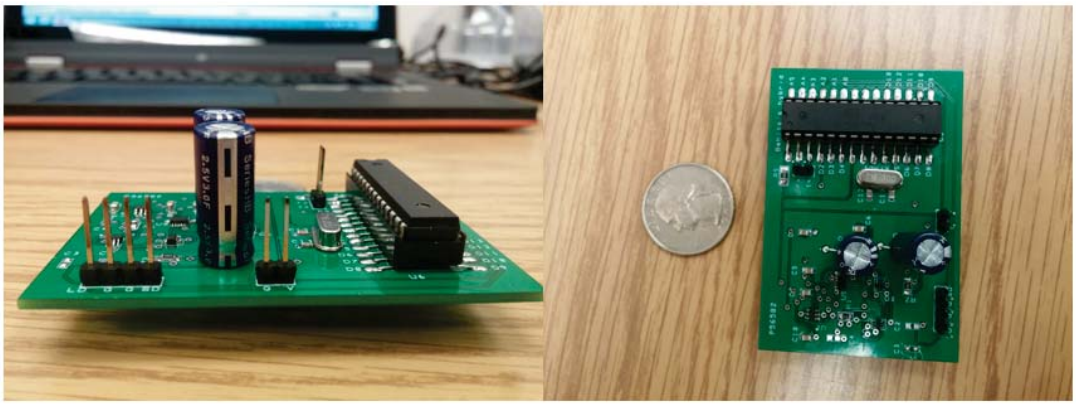

Figure 3.11. Built hybrid power system PCB

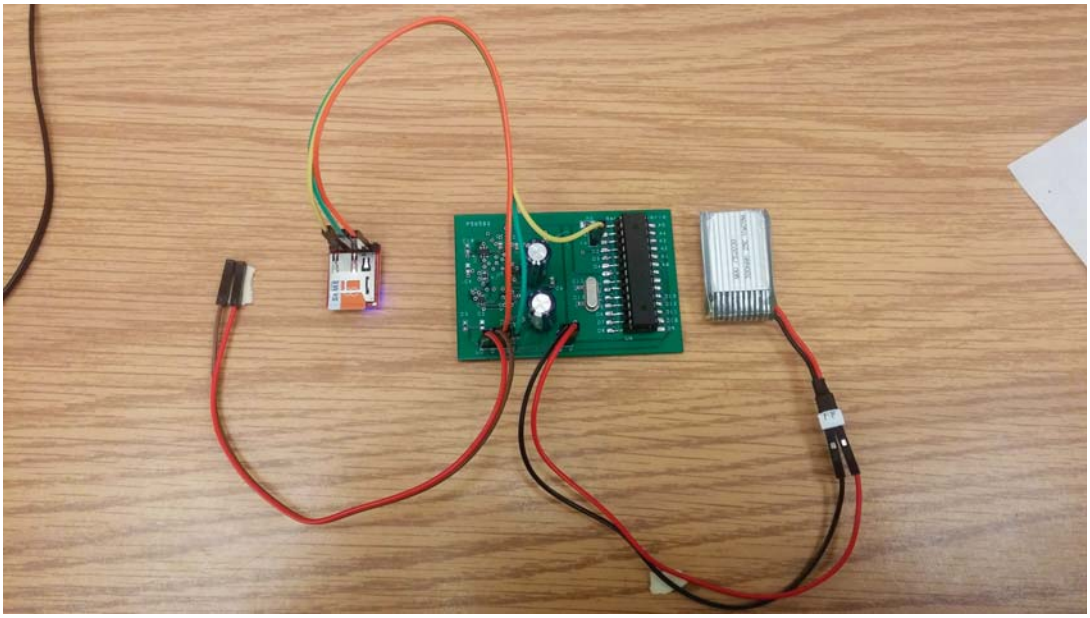

Figure 3.12. Built hybrid power system PCB connections layout

CHAPTER 4. EXPERIMENTS

4.1 Testbed Design

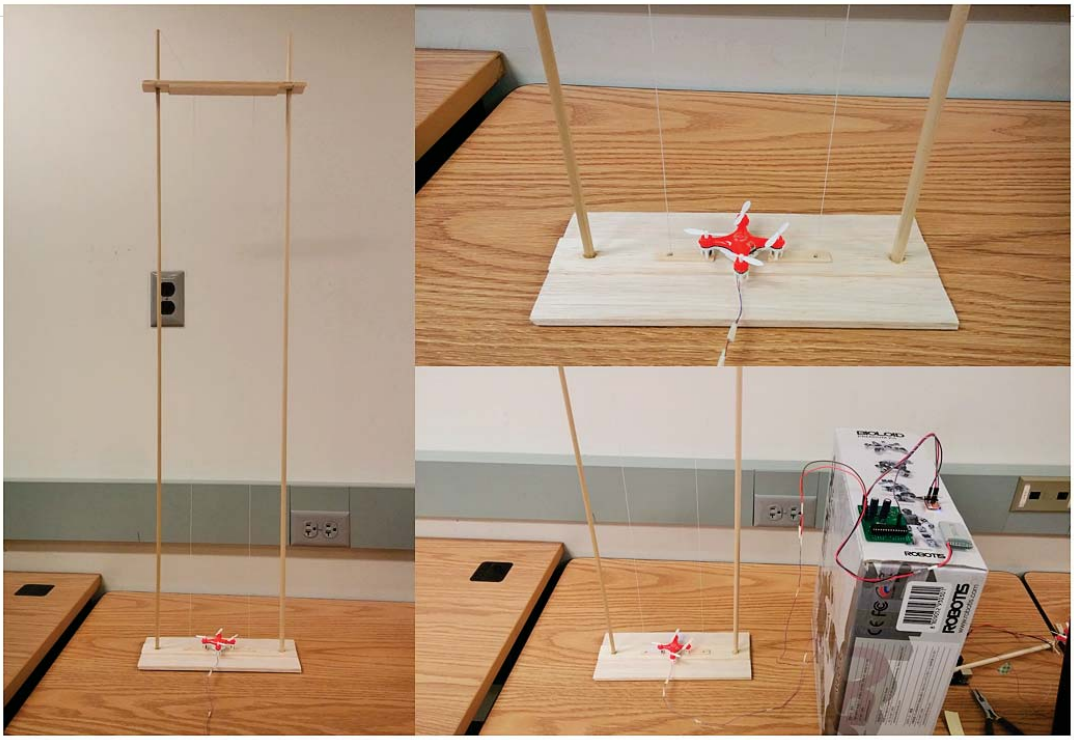

Figure 4.1. Testbed for Cheerson CX-10

Sometimes it is hard to control a quadcopter, especially for experimental purposes because an unsteady flight pattern can affect experimental data. To provide a safe flight to Cheerson CX-10, to reduce the risks of damage, and to decrease the lurking variables, a test bed was constructed (Roberts, 2013). The

testbed structure was made out of plywood, and thin wires were used to maintain vertical flight only. Dimensions of the testbed were 39x10x4 inch (Figure 4.1).

Figure 4.2. Modified Cheerson CX-10

The battery of Cheerson-CX10 was desoldered and replaced with power wires. After battery removal, the weight of the quadcopter was 10 grams. The bottom part of the quadcopter was glued to a flat plywood stick, which eliminates the risk of the propellers touching testbed wires (Figure 4.2). The designed hybrid power system was placed on top of an 18 inch box to reduce the weight of the power wires (Figure 4.1). After preparing the quadcopter for the flight, several tests were completed. Those tests will be explained in depth.

4.2 Test 1: SCAP Charge Time

Based on SCAP charge time Equation 3.3, a charge time for this system was calculated.

C_{out} = 1.5F, V_{cout} = 4.0V, V_{ini} = 2.34V, I_{out} = 0.15A.

$$t_{charge} = \frac{1.5F(4V - 2.34V)}{0.15} = 16.6sec \tag{4.1}$$

A simulation was done to check SCAP charge time. SCAP readings were recorded every 0.3 seconds (Figure 4.3). The calculated and simulated results were approximately the same. This means that the SCAPs take about 16 seconds to charge at the beginning of the system work and constantly recharge. Once SCAPs reach a threshold voltage level, LTC3225-1 automatically stops charging, preventing overvoltage and other damage to the system. The charger starts charging back when the threshold voltage drops. In this study the threshold voltage was 4.0V.

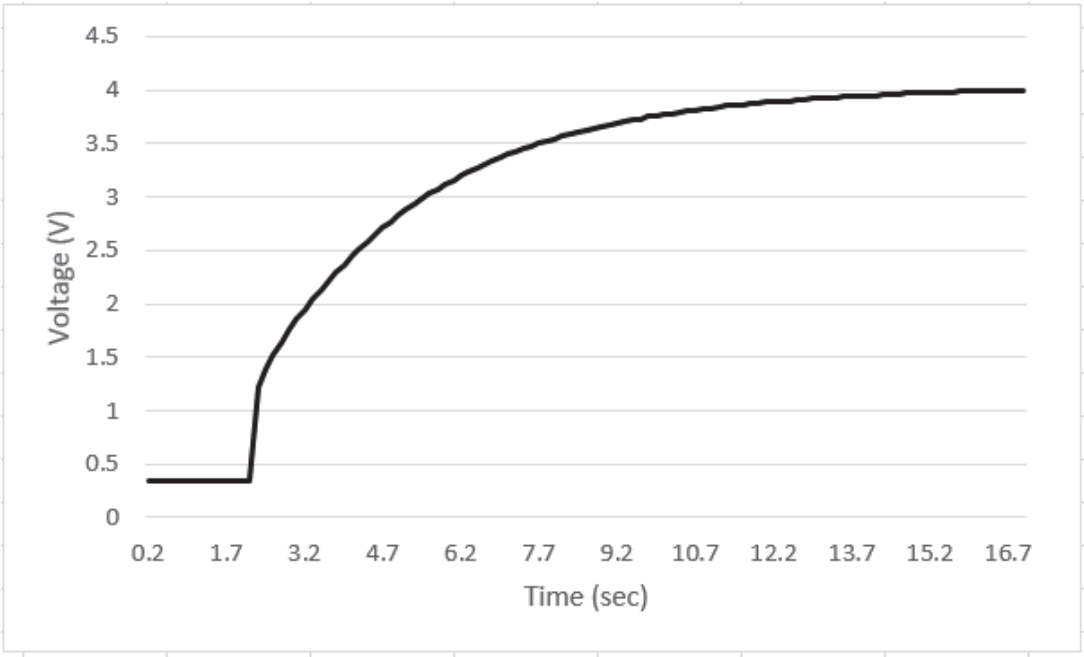

Figure 4.3. SCAP charge time

4.3 Test 2: Flight Time at a Specific Voltage Threshold

The 3.7V 300mAh Li-Po battery that was implemented in this study has 0.2C discharge rate and 3.0V cut-off voltage. Its voltage at a fully charged state is equal to 4.0 - 4.2V. A discharge of over 80% is considered a deep discharge that can decrease the battery life cycle and performance level (Fuller, Doyle, & Newman, 1994; Team, 2008). For this reason, for this test, 75% Depth of Discharge (DOD) was selected, which is 3.7V (Figure 4.4). So the quadcopter will fly until the battery voltage reaches 3.7V.

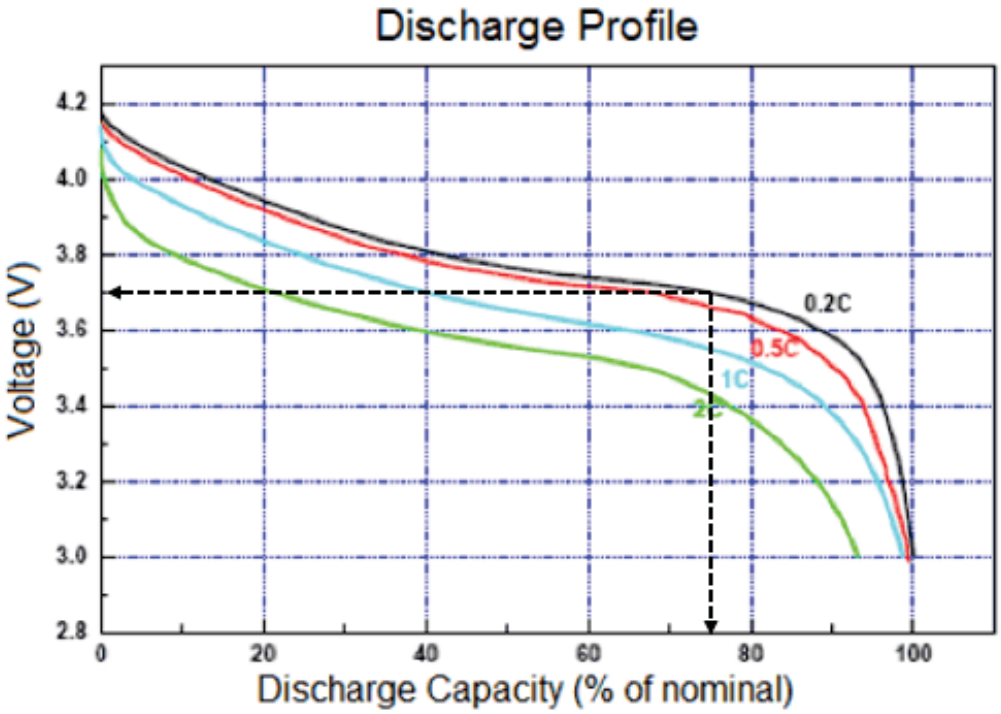

Figure 4.4. 3.7V Li-Po battery discharge profile

(*Li-Po Battery DOD*, n.d.)

The flight test was conducted on the built testbed using a joystick for speed control. Two speed modes were selected, which were slow and average. The speeds

were set based on the joystick button positions. it was decided to implement 10 seconds on average speed and 10 seconds on low speed flight pattern. Six fully charged batteries were used for the test, three for the battery powered system and three for the hybrid powered system. In total, 30 flight samples were made, 15 for the battery powered flight and 15 for the hybrid powered flight. The real time flight data was controlled and recorded using a CoolTerm serial port terminal.

4.3.1 Fixed Voltage Battery Powered MAV Flight Time

As was mentioned in the Methodology section, the LTC4411 power controlling switch is able to switch between two power sources. To power the load only from a battery, a simple code needs to be written for the microcontroller:

```
pinMode(ORpin, OUTPUT);
digitalWrite(ORpin, LOW);
int BATdata = analogRead(A0);
float BATvoltage = BATdata * (5 / 1023.0);
Serial.print("Vbat");
Serial.print(" ");
Serial.println(BATvoltage);
delay(500);
```

where ORpin is a CTL pin of LTC4411, which is responsible for switching power sources. When it is active LOW, the primary power source battery powers the load. When it is active HIGH, the auxiliary power source SCAP supplies the load. The microcontroller reads the battery voltage and prints it out every 0.5 seconds. As a result of the 15 flights, the following flight time data was collected (Table 4.1). The average flight time was 3.04 minutes.

Table 4.1
Fixed voltage battery powered MAV flight time

Number of flights	**Flight time (in sec)**	**Flight time (in min)**
1	151	2.51
2	263	4.38
3	240	3.99
4	156	2.59
5	197	3.28
6	111	1.85
7	202	3.36
8	166	2.77
9	207	3.45
10	182	3.03
11	229	3.82
12	117	1.94
13	202	3.36
14	179	2.98
15	135	2.25
Average flight time	**182.2**	**3.04**

4.3.2 Fixed Voltage Hybrid Powered MAV Flight Time

In this section of the test, both power sources had to supply the load. In order to determine what power source to turn on, a voltage of 3.6V was selected based on the voltage readings at the load (Figure 4.2). On the graph, the

quadcopter speed was controlled from low to high and the readings were recorded. As can be observed, the load at higher speeds require more voltage. So the 3.6V level was selected as a switching point to the SCAP supply. LTC4411 was programmed as follows:

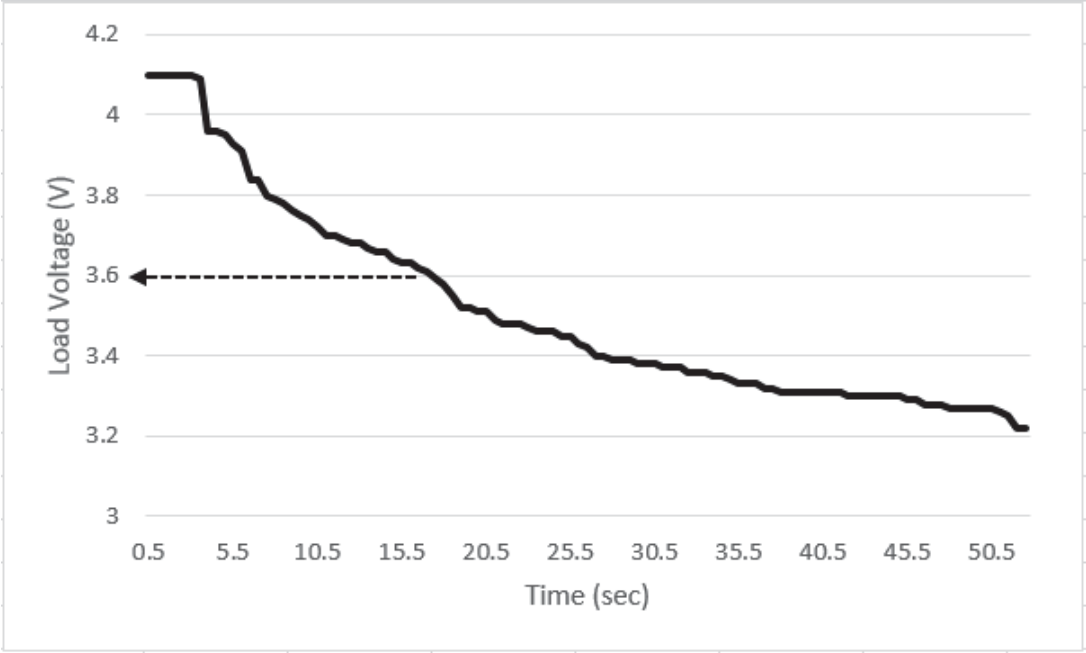

Figure 4.5. Voltage readings at the load

if (Vload >3.6)

{

pinMode(ORpin, OUTPUT);

digitalWrite(ORpin, HIGH);

int SCAPdata = analogRead(A0);

*float SCAPvoltage = SCAPdata * (5 / 1023.0);*

Serial.print("Vscap");

Serial.print(" ");

Serial.println(SCAPvoltage);

```
delay(500);
}

        else
{
pinMode(ORpin, OUTPUT);
digitalWrite(ORpin, LOW);
int BATdata = analogRead(A1);
float BATvoltage = BATdata * (5 / 1023.0);
Serial.print("Vbat");
Serial.print(" ");
Serial.println(BATvoltage);
delay(500);
}
```

where the CTL pin of LTC4411 was set to active HIGH when voltage at the load went above 3.6V; otherwise, the load continued to be supplied by the battery. Readings were recorded every 0.5 seconds, and 15 sample flights were done (Table 4.2). The average flight time was 6.26 minutes.

4.4 Test 3: Flight Time at a Fixed Speed

In this test stage, the quadcopter had to fly at a fixed speed. This eliminates joystick speed control errors due to the fact that the joystick speed cannot be set numerically. An average speed was chosen, which was the exact center point of the joystick toggle pin. Two flight modes were investigated, battery powered and hybrid powered. As was done in the seconds test, each flight was stopped when the battery voltage reached a 75% discharge rate. Voltage readings were recorded every second, and total flight time was collected for every flight. In total, 30 flights were done for two flight modes using six fully charged batteries.

Table 4.2
Fixed voltage hybrid powered MAV flight time

Number of flights	**Flight time (in sec)**	**Flight time (in min)**
1	265	4.42
2	420	6.99
3	451	7.52
4	374	6.23
5	393	6.55
6	401	6.68
7	391	6.52
8	345	5.75
9	429	7.15
10	386	6.43
11	255	4.24
12	397	6.62
13	284	4.73
14	420	7.00
15	427	7.12
Average flight time	**375.74**	**6.26**

4.4.1 Fixed Time Battery Powered Cheerson CX-10 Flight Time

For this flight mode, the microcontroller was programmed in a way that disables SCAPs and only enables a battery. This was accomplished by setting the CTL pin of LTC4411 to active LOW. The average flight time for this mode was 3.05 minutes (Table 4.3).

Table 4.3
Fixed speed battery powered Cheerson CX-10 flight time

Number of flights	**Flight time (in sec)**	**Flight time (in min)**
1	210	3.50
2	190	3.17
3	165	2.75
4	175	2.92
5	219	3.65
6	182	3.03
7	198	3.30
8	178	2.97
9	207	3.45
10	172	2.87
11	168	2.80
12	182	3.03
13	140	2.33
14	180	3.00
15	175	2.92
Average flight time	**183**	**3.05**

4.4.2 Fixed Time Hybrid Powered Cheerson CX-10 Flight Time

In this flight mode, the microcontroller was programmed to allow a battery to power the load for 10 seconds and then switch to SCAPs for 5 seconds. The reason 5 seconds was chosen for the SCAPs was to prevent a deep discharge of SCAPs. Again, the switching was controlled by the CTL pin of LTC4411. The average flight time was 3.86 minutes (Table 4.4).

Table 4.4
Fixed speed hybrid powered Cheerson CX-10 flight time

Number of flights	**Flight time (in sec)**	**Flight time (in min)**
1	222	3.70
2	246	4.10
3	265	4.42
4	248	4.13
5	258	4.30
6	198	3.30
7	202	3.37
8	219	3.65
9	225	3.75
10	254	4.23
11	241	4.02
12	206	3.43
13	219	3.65
14	241	4.02
15	228	3.80
Average flight time	**231**	**3.86**

CHAPTER 5. DATA ANALYSIS

5.1 Unit & Sampling

The following section discusses the statistical data analysis, which includes the hypotheses, population, samples, variables, and the measure for success. In this study, Two Sample T-Test was utilized because the data was assumed to be normally distributed and satisfied the Central Limit Theorem.

5.1.1 Hypotheses

The hypotheses for this study are the following:

H_0: The flight time of the hybrid powered MAV is the same as the flight time of the battery powered MAV ($\mu_1 = \mu_2$).

H_α: The flight time of the hybrid powered MAV is more than the flight time of the battery powered MAV ($\mu_1 > \mu_2$).

5.1.2 Population

Collected flight times were the population of the study.

5.1.3 Sample

The number of samples from the battery powered MAV was equal to $n_1 = 15$ and from the hybrid powered MAV was equal to $n_2 = 15$ with sample standard deviations s_1 and s_2.

5.1.4 Variables

The variable of the study was flight time.

5.1.5 Measure for Success

By looking at the advantages of SCUP, at least 5% ($\alpha = 0.05$) success was expected. The success rate was calculated by comparing the battery powered MAV results to the hybrid powered MAV results.

5.2 Statistical Analysis for Test 2

For more accurate results, seconds were used as the flight time unit. From the collected data in Test 2, these sample mean and standard deviations were calculated:

$x_1 = 375.74$

$x_2 = 182.2$

$s_1 = 61.61$

$s_2 = 43.99$

$$t = \frac{375.74 - 182.2}{\sqrt{\frac{61.61^2}{15} + \frac{43.99^2}{15}}} = 9.90 \tag{5.1}$$

The test statistics was equal to t = 9.90, giving P <0.0005, which is less than α. Taking this into consideration, the Null hypothesis was rejected, and it was concluded that the flight time of the hybrid powered MAV was more than the flight time of the battery powered MAV.

5.3 Statistical Analysis for Test 3

For more accurate results, seconds were used as the flight time unit. From the collected data in Test 3, these sample mean and standard deviations were calculated:

$x_1 = 231.47$

$x_2 = 182.73$

$s_1 = 20.86$

$s_2 = 19.92$

$$t = \frac{231.47 - 182.73}{\sqrt{\frac{20.86^2}{15} + \frac{19.92^2}{15}}} = 6.54 \tag{5.2}$$

The test statistics was equal to t = 6.54, giving P <0.0005, which is less than α. Taking this into consideration, the Null hypothesis was rejected, and it was concluded that the flight time of the hybrid powered MAV was more than the flight time of the battery powered MAV.

CHAPTER 6. CONCLUSIONS AND FUTURE WORK

In this study, a hybrid power system was designed, implemented, and tested. The hybrid power system board size was not designed for on board flight. However, a smaller version can be designed in the future. After board manufacturing, a testbed was built and three tests were conducted. Because this study was mainly focused on increasing the flight time of the MAVs, in two of the three experiments, flight time data were collected. The study statistically proved the hypothesis that the hybrid powered MAV flight time would be more than the battery powered flight time. However, it should be noted that the study only used voltage measurements and controlled power switches through looking just at voltage measurements.

In Test 2, the hybrid power system efficiency over the battery power system was equal to 106%. This shows that using the SCAP power for acceleration and power intensive flights is more efficient.

In Test 3, the hybrid power system efficiency over the battery power system was equal to 26%. This means that the hybrid power system is less efficient at steady speed flights.

In the future, more attention needs to be paid to the current and overall power consumption of the MAVs. This can be done by adding a current sensor to the PCB. Knowing all the electrical measurements controlling the two power sources would have been much easier. Also, a smaller version of the PCB needs to be designed and manufactured and tested on-board flights of MAVs. After all of these complete, a reasonable and firm conclusion can be made.

LIST OF REFERENCES

LIST OF REFERENCES

3.7V 300mAh Li-Po battery datasheet. (n.d.). Retrieved from `http://all-battery.com/datasheet`

ATmega328P microcontroller. (n.d.). Retrieved from `http://www.atmel.com`

Balasubramanian, K., Kolmanovsky, I., & Saha, B. (2012). Range maximization of a direct methanol fuel cell powered mini air vehicle using stochastic drift counteraction optimal control. In *American control conference (acc), 2012* (pp. 3272–3277).

Boddhu, S., Botha, H., McCurdy, B., Gallagher, J. C., & Matson, E. A. (2014). Research platform for flapping wing micro air vehicle control study. In *The 3rd international conference on robot intelligence technology and applications (rita 2014).*

BU-210: Fuel Cell Technology. (n.d.). Retrieved from `http://batteryuniversity.com/learn/article/fuel_cell_technology`

Camara, M. B., Gualous, H., Gustin, F., Berthon, A., & Dakyo, B. (2010). Dc/dc converter design for supercapacitor and battery power management in hybrid vehicle applicationspolynomial control strategy. *Industrial Electronics, IEEE Transactions on*, *57*(2), 587–597.

Cao, J., & Emadi, A. (2012). A new battery/ultracapacitor hybrid energy storage system for electric, hybrid, and plug-in hybrid electric vehicles. *Power Electronics, IEEE Transactions on*, *27*(1), 122–132.

Carter, R., & Cruden, A. (2008). Strategies for control of a battery/supercapacitor system in an electric vehicle. In *Power electronics, electrical drives, automation and motion, 2008. speedam 2008. international symposium on* (pp. 727–732).

Di Napoli, A., Crescimbini, F., Guilii Capponi, F., & Solero, L. (2002). Control strategy for multiple input dc-dc power converters devoted to hybrid vehicle propulsion systems. In *Industrial electronics, 2002. isie 2002. proceedings of the 2002 ieee international symposium on* (Vol. 3, pp. 1036–1041).

Dowling, K. (1997). *Power sources for small robots.* Carnegie Mellon University, the Robotics Institute.

Dual P-Channel MOSFET Si1965 datasheet. (n.d.). Retrieved from `http://vishay.com/docs/68765/SI1965DH`

Finio, B. M., Eum, B., Oland, C., & Wood, R. J. (2009). Asymmetric flapping for a robotic fly using a hybrid power-control actuator. In *Intelligent robots and systems, 2009. iros 2009. ieee/rsj international conference on* (pp. 2755–2762).

Fuller, T. F., Doyle, M., & Newman, J. (1994). Relaxation phenomena in lithium-ion-insertion cells. *Journal of the Electrochemical Society*, *141*(4), 982–990.

Gallagher, J. C., Matson, E., & Greenwood, G. (2014). Improvements to evolutionary model consistency checking for a flapping-wing micro air vehicle. In *the 2014 ieee international conference on evolvable systems (ices) (ices2014).*

Gallagher, J. C., Matson, E. T., & Greenwood, G. W. (2013). On the implications of plug-and-learn adaptive hardware components toward a cyberphysical systems perspective on evolvable and adaptive hardware. In *Evolvable systems (ices), 2013 ieee international conference on* (pp. 59–65).

Gao, L., Dougal, R. A., & Liu, S. (2005). Power enhancement of an actively controlled battery/ultracapacitor hybrid. *Power Electronics, IEEE Transactions on*, *20*(1), 236–243.

Goppert, J., Gomez, M., Kim, Y., Golden, L., Hwang, I., & Matson, E. (2014). Hybrid model checking using linear matrix inequalities applied to a self-balancing robot. In *The 3rd international conference on robot intelligence technology and applications (rita 2014).*

Goppert, J., Matson, E., & Hwang, I. (2015). Application of model checking to a fixed-wing uas subject to bounded disturbances. *AIAA Science and Technology Forum 2015 (SciTech 2015).*

Grama, A., Patarau, T., Etz, R., & Petreus, D. (2014). Simulink test bench for a hybrid battery-supercapacitor power system. In *Design and technology in electronic packaging (siitme), 2014 ieee 20th international symposium for* (pp. 153–156).

Greenwood, G., Gallagher, J., & Matson, E. (2015). Cyber-physical systems: The next generation of evolvable hardware research and applications. In *Proceedings of the 18th asia pacific symposium on intelligent and evolutionary systems, volume 1* (pp. 285–296).

HB Supercapacitor datasheet. (n.d.). Retrieved from `http://cooperindustries.com`

Jarushi, A., & Schofield, N. (2010). Battery and supercapacitor combination for a series hybrid electric vehicle. In *Power electronics, machines and drives (pemd 2010), 5th iet international conference on* (pp. 1–6).

Khaligh, A., & Li, Z. (2010). Battery, ultracapacitor, fuel cell, and hybrid energy storage systems for electric, hybrid electric, fuel cell, and plug-in hybrid electric vehicles: State of the art. *Vehicular Technology, IEEE Transactions on*, *59*(6), 2806–2814.

Li-Po Battery DOD. (n.d.).

LTC3225/LTC3225-1 Supercapacitor charger datasheet. (n.d.). Retrieved from `http://cds.linear.com/docs/en/datasheet/3225fb`

LTC4411 Ideal diode datasheet. (n.d.). Retrieved from `http://cds.linear.com/docs/en/datasheet/4411fa`

Lukic, S. M., Wirasingha, S. G., Rodriguez, F., Cao, J., & Emadi, A. (2006). Power management of an ultracapacitor/battery hybrid energy storage system in an hev. In *Vehicle power and propulsion conference, 2006. vppc'06. ieee* (pp. 1–6).

Ma, K. Y., Chirarattananon, P., Fuller, S. B., & Wood, R. J. (2013). Controlled flight of a biologically inspired, insect-scale robot. *Science*, *340*(6132), 603–607.

Ortúzar, M., Moreno, J., & Dixon, J. (2007). Ultracapacitor-based auxiliary energy system for an electric vehicle: Implementation and evaluation. *Industrial Electronics, IEEE Transactions on*, *54*(4), 2147–2156.

Pay, S., & Baghzouz, Y. (2003). Effectiveness of battery-supercapacitor combination in electric vehicles. In *Power tech conference proceedings, 2003 ieee bologna* (Vol. 3, pp. 6–pp).

Perseghetti, B., Gallagher, J. C., Goppert, J., Yantek, S., Matson, E., & Hwang, I. (2015). Optimizing energy efficiency of a flapping-wing robotic bird through application of evolutionary algorithms. *AIAA Science and Technology Forum 2015 (SciTech 2015)*.

Rafik, F., Gualous, H., Gallay, R., Crausaz, A., & Berthon, A. (2006). Supercapacitors characterization for hybrid vehicle applications. In *Power electronics and motion control conference, 2006. ipemc 2006. ces/ieee 5th international* (Vol. 3, pp. 1–5).

Roberts, D. (2013). Construction and testing of a quadcopter.

Sampaio, R. C. B., Hernandes, A. C., Becker, M., Catalano, F. M., Zanini, F., Nobrega, J. L., & Martins, C. (2014). Novel hybrid electric motor glider-quadrotor mav for in-flight/v-stol launching. In *Aerospace conference, 2014 ieee* (pp. 1–12).

Sparkfun OpenLog. (n.d.). Retrieved from `https://www.sparkfun.com/products/9530`

Team, M. E. V. (2008). A guide to understanding battery specifications. *Academia.edu*.

Vilathgamuwa, D., Jayasinghe, S., Lee, F., & Madawala, U. (2011). A unique battery/supercapacitor direct integration scheme for hybrid electric vehicles. In *Iecon 2011-37th annual conference on ieee industrial electronics society* (pp. 3020–3025).

Wilhelm, A., Surgenor, B., & Pharoah, J. (2005). Evaluation of a micro fuel cell as applied to a mobile robot. In *Mechatronics and automation, 2005 ieee international conference* (Vol. 1, pp. 32–36).

Wood, R. J. (2007). Liftoff of a 60mg flapping-wing mav. In *Intelligent robots and systems, 2007. iros 2007. ieee/rsj international conference on* (pp. 1889–1894).

Zhang, Y., Jiang, Z., & Yu, X. (2008). Control strategies for battery/supercapacitor hybrid energy storage systems. In *Energy 2030 conference, 2008. energy 2008. ieee* (pp. 1–6).